RESEARCH ARTICLE



Check for updates

Effects of experimental nitrogen deposition on soil organic carbon storage in Southern California drylands

Johann F. Püspök¹ | Sharon Zhao¹ | Anthony D. Calma¹ | George L. Vourlitis² | Steven D. Allison^{3,4} | Emma L. Aronson⁵ | Joshua P. Schimel⁶ | Erin J. Hanan⁷ Peter M. Homvak¹

²Department of Biological Sciences, California State University, San Marcos. California, USA

³Department of Ecology and Evolutionary Biology, University of California, Irvine, California, USA

⁴Department of Earth System Science, University of California, Irvine, California,

⁵Department of Microbiology and Plant Pathology, University of California, Riverside, California, USA

⁶Department of Ecology, Evolution, and Marine Biology and Earth Research Institute, University of California, Santa Barbara, California, USA

⁷Department of Natural Resources and Environmental Science, University of Nevada, Reno, Nevada, USA

Correspondence

Johann F. Püspök, Department of Environmental Sciences, University of California, Riverside, CA 92521, USA. Email: johann.puespoek@email.ucr.edu

Funding information

National Science Foundation, Grant/ Award Number: DEB 1916622; U.S. Department of Energy, Grant/Award Number: DE-SC0020382

Abstract

Atmospheric nitrogen (N) deposition is enriching soils with N across biomes. Soil N enrichment can increase plant productivity and affect microbial activity, thereby increasing soil organic carbon (SOC), but such responses vary across biomes. Drylands cover ~45% of Earth's land area and store ~33% of global SOC contained in the top 1 m of soil. Nitrogen fertilization could, therefore, disproportionately impact carbon (C) cycling, yet whether dryland SOC storage increases with N remains unclear. To understand how N enrichment may change SOC storage, we separated SOC into plant-derived, particulate organic C (POC), and largely microbially derived, mineralassociated organic C (MAOC) at four N deposition experimental sites in Southern California. Theory suggests that N enrichment increases the efficiency by which microbes build MAOC (C stabilization efficiency) if soil pH stays constant. But if soils acidify, a common response to N enrichment, then microbial biomass and enzymatic organic matter decay may decrease, increasing POC but not MAOC. We found that N enrichment had no effect on C fractions except for a decrease in MAOC at one site. Specifically, despite reported increases in plant biomass in three sites and decreases in microbial biomass and extracellular enzyme activities in two sites that acidified, POC did not increase. Furthermore, microbial C use and stabilization efficiency increased in a non-acidified site, but without increasing MAOC. Instead, MAOC decreased by 16% at one of the sites that acidified, likely because it lost 47% of the exchangeable calcium (Ca) relative to controls. Indeed, MAOC was strongly and positively affected by Ca, which directly and, through its positive effect on microbial biomass, explained 58% of variation in MAOC. Long-term effects of N fertilization on dryland SOC storage appear abiotic in nature, such that drylands where Ca-stabilization of SOC is prevalent and soils acidify, are most at risk for significant C loss.

KEYWORDS

atmospheric nitrogen deposition, carbon use efficiency, extracellular enzymes, fertilization, mineral-associated organic matter (MAOM), particulate organic matter (POM), soil acidification, soil microbes

¹Department of Environmental Sciences, University of California, Riverside, California, USA

1 | INTRODUCTION

Atmospheric nitrogen (N) deposition has tripled since 1850 due to emissions from agriculture and fossil fuel burning, leading to a global enrichment of soil N pools (Gruber & Galloway, 2008; Kanakidou et al., 2016). This N enrichment affects plant growth and microbial activity and, thereby, strongly interacts with the global carbon (C) cycle (Gruber & Galloway, 2008; O'Sullivan et al., 2019; Treseder, 2008). Soil organic C (SOC) contains more C than vegetation and the atmosphere combined and confers important soil functions such as soil fertility and water retention (Weil & Brady, 2017). Globally, SOC pools have increased by 4.2% in response to N enrichment (Xu et al., 2021), but responses can be biome-specific (Deng et al., 2020). Drylands make up ~45% of the global land area and store up to 33% of the global SOC stocks contained in the top 1m of soil (Plaza, Zaccone, et al., 2018; Prăvălie, 2016). Therefore, dryland response to N deposition could have substantial consequences on global C cycling and soil quality (Homyak et al., 2014; Osborne et al., 2022; Plaza, Gascó, et al., 2018), but they are underrepresented in global analyses evaluating N fertilization effects on soil C storage (Xu et al., 2021). While both increases and decreases in SOC have been measured along N deposition gradients in drylands (Maestre et al., 2016; Ochoa-hueso et al., 2013), the magnitude of and mechanisms behind dryland C storage change in response to N deposition remain unclear.

The effects of N enrichment on SOC storage depend on many factors including changes in plant C inputs, organic matter decomposition, microbial transformations of C compounds, and stabilization of C through interactions with soil minerals (Castellano et al., 2015; Janssens et al., 2010; Ye et al., 2018). To help identify changes in SOC storage and the mechanisms governing the fate of C in response to N deposition, SOC can be separated into two pools of different origin and persistence (Lavallee et al., 2020): (i) a relatively fast cycling, particulate organic C (POC) fraction, consisting of relatively undecomposed plant material, and (ii) a relatively slow cycling, mineral-associated organic C (MAOC) fraction, consisting of heavily decomposed plant compounds and microbial products (Lavallee et al., 2020; Whalen et al., 2022). Due to their differences in formation, variation in the largely plant-derived POC fraction is thought to depend mostly on N-induced changes in decomposition and plant biomass production (Rossi et al., 2020), with roots considered important in drylands where much of aboveground biomass can decompose before being incorporated into the soil (Berenstecher et al., 2021). In contrast, variation in MAOC is thought to depend more on changes in litter quality, microbial metabolism, and soil sorption potential (Figure 1) (Castellano et al., 2015; Sokol et al., 2019). Previous research separating SOC into POC and MAOC has shown that N fertilization effects on C storage in semi-arid grasslands were mostly driven by increased aboveground biomass and POC, but microbial C cycling and mineral stabilization in the MAOC pool may be also important (Lin et al., 2019; Ye et al., 2018).

Microbial C cycling can affect MAOC pools through the in-vivo transformation of C compounds—also known as the "microbial C

pump"-into microbial biomass and microbial by-products (Liang et al., 2017). Carbon that cycles through the "pump" via microbial death or exudation can then associate with mineral surfaces and become protected from further microbial decomposition (Islam et al., 2022). Therefore, microbial C use efficiency (CUE), the fraction of C uptake that is allocated to biomass growth, is key to determining SOC storage (Bradford et al., 2013). Microbial CUE is often measured by tracing microbial uptake and respiration of isotopically-labelled C compounds, which depends on many factors including microbial community composition, climate, soil physicochemical conditions, and soil nutrient status (Butcher et al., 2020; Jones et al., 2019; Manzoni et al., 2012; Pold et al., 2020). Microbial Cstabilization efficiency (CSE) extends the CUE term by accounting for the formation of microbial residues that can be stabilized in soil, and can thus link N-induced changes in microbial physiology with long-term C stabilization, particularly when measured over longer time periods (e.g., multiple weeks) (Geyer et al., 2020). Studies in temperate grasslands found that adding N increased CUE and SOC storage (Poeplau et al., 2019). However, in drylands, microbes may be limited by C or there may be no link between CUE and MAOC formation because dryland soils are typically coarse-textured with low C sorption potential (Cai et al., 2022; Creamer et al., 2014, 2016; Schaeffer et al., 2003). How microbial CSE or CUE change in response to N enrichment has not been measured before in drylands, and it is not known whether atmospheric N deposition can affect SOC storage via changes to the microbial C pump.

The effects of atmospheric N deposition on SOC storage may also depend on whether N enrichment acidifies soils. For example, ecosystem models suggest N enrichment should favor the transformation of POC into persistent MAOC, but only if decomposition is N-limited and soils do not become too acidic to adversely affect microbial physiology (Averill & Waring, 2018). However, acidification is a common response to N enrichment resulting from H⁺ release during nitrification, H⁺ release after plants take up NH₄⁺, and leaching of base cations as companion ions to NO₃⁻ (Tian & Niu, 2015). Thus, many studies attribute increases in SOC after N enrichment to acidity-induced decreases in microbial biomass and decreased organic matter decomposition, which lead to a build-up of POC without further breakdown to MAOC (Janssens et al., 2010; O'Sullivan et al., 2019; Riggs & Hobbie, 2016; Treseder, 2008). Notably, even more alkaline drylands, considered to be well-buffered against changes in pH (Slessarev et al., 2016), can acidify even in nonexperimental settings (Yang et al., 2012). Identifying which mechanism governs SOC dynamics has, therefore, been challenging. One way to overcome this challenge is to measure changes in the activity of extracellular enzymes. Because decomposition and changes in SOC are largely driven by enzymes that break down polymers into smaller, more easily assimilated compounds (Burns et al., 2013), extracellular enzyme activities may offer an opportunity to disentangle whether acidification affects microbial decomposition (e.g., a decrease in decomposition may correlate with reduced enzyme activity), the partitioning of SOC, and the fate of both POC and MAOC pools.

FIGURE 1 Conceptual overview of the processes that form soil organic C (SOC) as POC and mineral-associated organic C (MAOC) at our site. Above- and belowground litter is stored as POC in soils. A fraction of aboveground litter is photochemically degraded aboveground and microbially decomposed to CO_2 before it can be stored as POC. POC is relatively accessible to microbes in soils and can be decomposed via the microbial C pump to form MAOC (Liang et al., 2017). A fraction of the POC decomposed by microbes is respired as CO_2 during microbial metabolism. In dryland soils, calcium (Ca^{2+}) is important in bridging negatively charged C compounds to negatively charged mineral surfaces to form MAOC. Nitrogen enrichment can affect C storage by affecting microbial decomposition of POC and its transformation into MAOC (blue arrow). Furthermore, nitrogen enrichment can acidify soils and destabilize MAOC as Ca^{2+} is leached, making the C vulnerable to microbial decomposition (orange arrows). Arrow thickness represents the relative strength of the C flux between pools. [Colour figure can be viewed at wileyonlinelibrary.com]

Beyond the direct effects of acidification on microbial physiology, and cascading effects on POC and MAOC pools, MAOC may change directly in response to changes in soil physicochemical conditions. For example, whether MAOC persists in soil largely depends on the number of sorption sites available for binding C (Castellano et al., 2015; Cotrufo et al., 2019). In dryland soils, SOC stabilization is thought to be primarily controlled by clay content and exchangeable calcium (Ca) (Rasmussen et al., 2018), as polyvalent cations, like Ca, can stabilize SOC by bridging negatively charged C compounds with negatively charged mineral surfaces or by binding together multiple

organic molecules (Rowley et al., 2018). In fact, N enrichment can destabilize Ca-bridges and MAOC via Ca leaching from acidification (Wan et al., 2021; Ye et al., 2018), but it is unclear how widespread such pH-induced MAOC losses are in relatively well-buffered dryland soils.

Long-term N fertilization experiments are powerful tools for understanding how N fertilization and changes in soil physicochemical properties may influence SOC dynamics, because they add known amounts of N while reducing natural variation in confounding factors (e.g., plant species, soil taxonomy, climate, etc.)

often present in studies along natural N deposition gradients. In this study, we use four sites in long-running (i.e., >13 years) N fertilization experiments across drylands in Southern California: one grassland site, two sites in deciduous shrub-dominated coastal sage scrub (CSS), and one site in evergreen shrub-dominated chaparral. Three of the four studied sites increased in AGB in response to N fertilization (Parolari et al., 2012; Vourlitis, Jaureguy, et al., 2021). To study how N enrichment and acidification may differently affect SOC fractions, two of the sites were fertilized with urea, NH₄⁺, and NO₃⁻, and showed calcium leaching and strong acidification, whereas the two other sites were fertilized with CaNO3 to prevent acidification. Specifically, we ask: How does long-term N fertilization affect C storage in POC and MAOC fractions under acidifying versus non-acidifying conditions? And does N fertilization change the stabilization efficiency of labile C inputs via the microbial C pump?

We answered these questions using a combination of size and density fractionations to separate soils into POC and MAOC pools. To explore which mechanisms may control changes in soil C fractions, we measured changes in exchangeable Ca as an index for how C stabilization potential was affected by N fertilization, and microbial biomass and enzyme activities as an index for how microbial decomposition was affected by N fertilization. Furthermore, we assessed C stabilization efficiency (CSE) and CUE by measuring the efficiency by which microbes retained ¹³C-labelled glucose in soil, during both short- and long-term incubations. We hypothesized that (a) the previously reported increase in plant growth in response to N addition at three of the sites (Parolari et al., 2012; Vourlitis, Jaureguy, et al., 2021) would increase POC, particularly in acidified plots where decomposition might be inhibited; (b) N enrichment would increase CSE and the transformation of POC into MAOC in non-acidified

plots; and (c) N enrichment would decrease exchangeable Ca and MAOC in acidified plots.

2 | MATERIALS AND METHODS

2.1 | Sites description

Our study was conducted at three long-running N fertilization experiments in Southern California that together consist of four sites and represent the three dominant vegetation types in the region: chaparral, CSS, and grassland. The chaparral site (CHAP) is located at the Sky Oaks Field Station in San Diego County, CA (33.381 N, 116.626 W, elev. 1420 m). The first CSS site (CSS1) is located at the Santa Margarita Ecological Reserve in Riverside County, CA (33.438 N, 117.181 W, elev. 248 m). The grassland site (GRASS) and second CSS site (CSS2) are part of the Loma Ridge Global Change Experiment located at Irvine Ranch National Landmark in Orange County, California (33.742 N, 117.704 W, elev. 365 m). All sites have a Mediterranean climate with cool, wet winters and hot, dry summers; most rain falls between November and April. Important site information is summarized in Table 1 and described in more detail below.

CHAP and CSS1 are extensively described in Vourlitis, Jaureguy, et al. (2021). Mean annual precipitation at CHAP is 382 mm. Vegetation is dominated by *Adenostoma fasciculatum* and *Ceanothus greggii*. Soils are Entic Ultic Haploxerolls (Sheephead series) derived from micaceous shist and have a loamy sand texture (Table S2). The site burned at the onset of the N fertilization experiment in 2003. CHAP experienced severe acidification in response to N fertilization, with soil pH decreasing by 1.65 pH units below control plots in 2021 (Table 2). Mean annual precipitation at CSS1 is 414 mm. Vegetation is

TABLE 1 Site description

	MAP (mm)	Dominant vegetation cover type	Fire history	Soil texture class	Background N deposition (kg N ha ⁻¹ year ⁻¹)	N fertilization rate (kg N ha ⁻¹ year ⁻¹)	Form of N added	Duration of N fertilization (years)
СНАР	382	Evergreen shrubland	Burned 2003	Loamy sand	2-4	50	NH ₄ NO ₃ (2003–2007) (NH ₄)2SO ₄ (2007–2009) Urea (2009–present)	17-18
CSS1	414	Drought- deciduous shrubland	No data	Sandy loam	2-4	50	NH ₄ NO ₃ (2003–2007) (NH ₄)2SO ₄ (2007–2009) urea (2009-present)	17-18
GRASS	281	Annual grassland	Burned 2007 and 2020	Sandy loam	15	60	CaNO ₃	13-14
CSS2	281	Drought- deciduous shrubland	Burned 2007 and 2020	Sandy loam	15	60	CaNO ₃	13-14

Note: MAP is mean annual precipitation. Information presented in this table is derived from Fenn et al. (2010), Khalili et al. (2016), Potts et al. (2012) and Vourlitis, Jaureguy, et al. (2021).

TABLE 2 Soil characteristics

	Soil pH		Sand fraction C (mg g ⁻¹)		Soil organic C (mg g ⁻¹)		Soil organic N (mg g ⁻¹)		
	Control	N added	Control	N added	Control	N added	Control	N added	
Dry season (Octob	er 2020)								
CHAP									
Shrub	6.52 (0.18)	4.89 (0.37)	1.98 (0.32)	1.88 (0.42)	13.58 (1.66)	12.49 (3.36)	0.57 (0.1)	0.56 (0.14)	
Inter-space	6.51 (0.16)	5.22 (0.29)	1.84 (0.52)	1.56 (0.28)	9.63 (1.07)	8.68 (1.09)	0.39 (0.04)	0.42 (0.08)	
CSS1									
Shrub	6.52 (0.12)	5.36 (0.22)	0.57 (0.19)	0.80 (0.13)	12.92 (3.21)	13.38 (1.89)	0.85 (0.20)	0.92 (0.12)	
Inter-space	6.58 (0.13)	5.91 (0.56)	0.69 (0.37)	0.93 (0.41)	12.54 (6.94)	13.23 (4.71)	0.82 (0.44)	0.91 (0.30)	
GRASS	6.44 (0.09)	6.39 (0.17)	0.98 (0.29)	1.13 (0.46)	14.34 (1.99)	14.11 (2.15)	1.33 (0.17)	1.32 (0.15)	
CSS2	6.31 (0.13)	6.59 (0.10)	0.53 (0.11)	0.61 (0.16)	13.57 (2.03)	14.29 (1.20)	1.09 (0.15)	1.15 (0.12)	
Wet season (April	2021)								
CHAP									
Shrub	6.64 (0.35)	4.90 (0.11)	1.98 (0.26)	1.77 (0.23)	15.90 (4.07)	13.44 (3.59)	0.65 (0.20)	0.63 (0.19)	
Inter-space	6.63 (0.26)	5.07 (0.25)	1.98 (0.31)	1.91 (0.41)	13.03 (3.91)	8.68 (0.56)	0.61 (0.29)	0.39 (0.09)	
CSS1									
Shrub	6.53 (0.19)	5.20 (0.46)	0.74 (0.34)	0.54 (0.09)	16.17 (4.88)	11.89 (3.08)	1.16 (0.35)	0.97 (0.31)	
Inter-space	6.82 (0.25)	5.17 (0.13)	0.50 (0.07)	0.58 (0.21)	11.73 (4.78)	12.50 (3.39)	0.82 (0.32)	0.99 (0.32)	
GRASS	6.31 (0.23)	6.58 (0.17)	0.80 (0.17)	0.95 (0.17)	13.65 (1.02)	13.69 (2.37)	1.22 (0.11)	1.25 (0.23)	
CSS2	6.55 (0.36)	6.61 (0.20)	0.68 (0.07)	0.57 (0.06)	14.78 (2.20)	15.37 (3.22)	1.22 (0.15)	1.29 (0.26)	

Note: Values are means (standard deviation; n=4). Numbers in bold indicate significant differences between control and N-fertilized plots evaluated in a three-way ANOVA across seasons and microhabitats for CHAP and CSS1, but in a two-way ANOVA across seasons for GRASS and CSS2 (p < .1). For NH₄⁺ and NO₃⁻, ANOVAs were performed on aligned rank transformed data to account for non-normality and unequal variances. WEOC is water-extractable organic C.

dominated by Artemisia californica and Salvia mellifera. Soils are Typic Rhodoxeralfs formed from weathered Gabbro material (Las Posas series) and have a sandy loam texture (Table S2). CSS1 experienced severe acidification in response to N fertilization, with soil pH decreasing by 1.49 pH units below control plots in 2021 (Table 2). CHAP and CSS1 have the same experimental layout, consisting of eight plots in four pairs. Each pair consists of one 10×10 m control plot and one 10×10 m N-fertilized plot. Plots have been fertilized with 50kg Nha $^{-1}$ year $^{-1}$ every fall since 2003 as either NH $_4$ NO $_3$ (2003–2007), (NH $_4$) $_2$ SO $_4$ (2007–2009), or urea (2009–present). Background N deposition rate at both sites is estimated as 2–4kg Nha $^{-1}$ year $^{-1}$ (Fenn et al., 2010).

Vegetation at the Loma Ridge Global Change Experiment consists of a mosaic of non-native annual grassland and CSS and hosts the GRASS and CSS2 sites. Mean annual precipitation is 281 mm (Khalili et al., 2016). Vegetation at GRASS mostly includes *Bromus diandrus*, *Lolium multiflorum* and *Avena fatua*. Abundant species at CSS2 include *Malosma laurina*, A. *californica* and S. *mellifera* (Potts et al., 2012). Soils are Typic Palexeralfs (Myford series) formed on colluvial deposits from sedimentary rocks and have a sandy loam texture (Khalili et al., 2016). GRASS and CSS2 have the same randomized split-plot design, consisting of four replicate plots that are split: half unfertilized and half fertilized with 60 kg N ha⁻¹ year⁻¹. Plots have been fertilized since 2007 with 20 kg N ha⁻¹ year⁻¹ as immediate-release CaNO₃ prior to the wet season and 40 kg N ha⁻¹ year⁻¹ as 100-day release CaNO₃ during the wet season. Background atmospheric

N deposition is estimated as $15\,kg\,N\,ha^{-1}$ year $^{-1}$ (Fenn et al., 2010). Fires burned the plots when fertilization started in 2007 and again in October 2020. The 2020 fire had no effect on soil bacterial community composition, microbial biomass or soil pH (Barbour et al., 2022; this study).

2.2 | Soil sampling

Soils at all sites were sampled at the end of the dry season in October 2020, when most plants are senesced, and at the end of the wet season in April 2021, when most plants are actively growing. After removing plant litter from the soil surface, two soil sub-samples were taken from each plot using a soil auger (2.54cm diameter ×10cm depth) and combined into one composite sample. Soil samples were taken from randomly selected locations in the plots at GRASS and from underneath randomly selected shrubs in the plots at CHAP, CSS1 and CSS2. At CHAP and CSS1, additional soil samples were taken from locations with bare soil in the interspaces between shrub canopies, yielding one "Beneath shrub" and one "Interspace" sample per plot. No interspace samples were taken at GRASS and CSS2 since there was no significant area of bare soil without plant cover. We took samples from beneath shrubs and interspaces where possible because we expected biological processes more important in driving the response to N fertilization beneath shrubs and abiotic processes more important in interspaces. Soil samples were brought

Soil organic C:N		WEOC (µgg ⁻¹)		NH ₄ ⁺ (μgg ⁻¹)		NO ₃ - (μgg ⁻¹)	$NO_3^-(\mu g g^{-1})$		
Control	N added	Control	N added	Control	N added	Control	N added		
28.36 (3.45)	25.95 (1.21)	88.39 (10.80)	70.60 (8.46)	0.57 (0.22)	11.98 (18.14)	0.08 (0.06)	1.00 (0.74)		
28.73 (3.76)	24.67 (2.36)	61.17 (7.43)	51.83 (14.73)	0.60 (0.09)	2.78 (1.89)	0.21 (0.12)	1.52 (1.00)		
20.70 (0.70)	24.07 (2.00)	01.17 (7.40)	31.00 (17.70)	0.00 (0.07)	2.70 (1.07)	5.21 (0.12)	1.52 (1.00)		
17.66 (0.66)	16.98 (0.53)	165.46 (41.85)	176.09 (34.35)	1.44 (0.28)	6.81 (3.43)	0.87 (0.35)	1.33 (0.68)		
17.48 (0.86)	16.73 (0.75)	154.44 (43.87)	160.32 (18.73)	2.21 (1.65)	4.08 (1.83)	1.18 (0.26)	3.13 (3.47)		
12.61 (0.42)	12.45 (0.75)	131.33 (22.61)	129.30 (22.86)	2.55 (2.62)	4.84 (3.98)	8.16 (4.21)	26.07 (7.25)		
14.46 (0.38)	14.58 (0.80)	133.08 (18.72)	161.79 (27.80)	0.79 (0.26)	0.95 (0.31)	0.79 (0.31)	1.62 (0.24)		
29.44 (4.19)	24.97 (1.78)	37.94 (7.24)	51.08 (25.62)	0.40 (0.21)	6.90 (4.22)	0.06 (0.10)	12.72 (5.84)		
27.68 (5.58)	27.37 (5.28)	20.25 (8.58)	17.84 (5.80)	0.45 (0.29)	9.04 (8.44)	0.06 (0.08)	7.27 (4.61)		
16.30 (1.19)	14.51 (1.17)	85.47 (23.95)	124.73 (62.75)	0.81 (0.27)	6.92 (4.50)	0.76 (0.55)	19.43 (10.80)		
16.51 (0.58)	15.01 (1.63)	83.10 (21.17)	91.70 (30.06)	1.70 (1.08)	3.19 (2.18)	3.83 (4.80)	42.42 (10.97)		
13.11 (0.45)	12.79 (0.32)	81.63 (4.71)	137.57 (95.55)	0.97 (0.22)	1.50 (0.25)	0.60 (0.23)	3.43 (1.00)		
14.11 (0.71)	13.89 (0.47)	83.79 (22.43)	74.20 (12.55)	1.79 (0.70)	2.37 (0.70)	3.81 (2.21)	14.26 (5.14)		

to the lab and sieved (2 mm) for all further analyses. Field-moist soil samples were kept at 4°C. All measurements on field-moist soil samples were done within 1 week of sampling to minimize storage effects. Gravimetric water content was measured by drying field-moist soil samples at 104°C for 24h. All data are expressed on a per g dry weight basis.

2.3 | Total C and N, soil pH, exchangeable Ca^{2+} , exchangeable NO_3^- and NH_4^+ and water-extractable organic C

The total soil C and N content was measured after combustion using a Flash EA 1112 NC analyzer (Thermo Fisher Scientific Inc.). Soil pH was measured with a glass electrode on air-dried soil in nanopure water (1:2 (w:v) soil dry weight:solution). Exchangeable Ca $^{2+}$ was measured in 0.1 M BaCl $_2$ extracts of air-dried soil (1:20 soil dry weight:solution) by inductively-coupled plasma optical-emission spectrometry (ICP–OES) using an Optima 7300 DV (Perkin-Elmer Inc.) (Hendershot & Duquette, 1986). Exchangeable nitrate (NO $_3^-$) and ammonium (NH $_4^+$) were measured in 2 M KCl extracts of field-moist soil (1:10 [w:v] soil dry weight:solution) on an AQ2 Discrete Analyzer (SEAL Analytical). Values below the limit of detection of the instrument were replaced with 0.003 mgNl $^{-1}$ for NO3– and 0.05 mgNl $^{-1}$ for NH4+. Water-extractable organic C (WEOC) was measured in nanopure water extracts of field-moist soil (1:10 [w:v]

soil dry weight:solution) on a TOC-V_{CHS} analyzer (Shimadzu). All analyses were conducted at the Environmental Sciences Research Laboratory (ESRL) at UC Riverside (https://envisci.ucr.edu/research/environmental-sciences-research-laboratory-esrl).

2.4 | Microbial biomass C and N

Microbial biomass C and N were measured with a chloroform slurry extraction (Fierer, 2003). Subsamples of 10g field-moist soil were shaken in 40ml 0.5 M $\rm K_2SO_4$ with or without addition of 0.5 ml chloroform. Chloroform was purged from the extracts by bubbling with room air for 30min. Extracts were filtered (0.9 μ m pore size) and analyzed for organic C and N on a TOC-V_{CHS} analyzer coupled with a TNM-1 Total nitrogen measuring unit (Shimadzu) in the ESRL. Microbial biomass C and N were calculated as the difference in organic C or N between subsamples extracted with and without chloroform (Brookes et al., 1985; Vance et al., 1987). No correction factor for extraction efficiency was used and thus we report a "flush" in microbial biomass C after extraction.

2.5 | Soil hydrolytic extracellular enzyme activities

Potential extracellular soil enzyme activities (see Table 3 for their function) were measured with fluorigenic substrates (Marx et al., 2001)

as described in the Supporting Information and paired accordingly: (i) α -glucosidase (AG) with 4-methylumbelliferyl- α -D-glucopyranoside; (ii) 1,4- β -cellobiohydrolase (CBH) with 4-MUF- β -D-cellobioside; (iii) β -glucosidase (BG) with 4-methylumbelliferyl β -D-glucopyranoside; (iv) N-acetyl- β -D-glucosaminidase (NAG) with 4-methylumbelliferyl N-acetyl- β -D-glucosaminide; (v) phosphomonoesterase with 4-methylumbelliferyl phosphate; and (vi) L-Leucine aminopeptidase (LAP) with L-Leucine-7-amido-4-methylcoumarin.

2.6 | Soil organic matter fractionation

Soil organic matter was fractionated into POC, sand-associated organic C, and silt and clay-associated organic C using a combination of density and size fractionation modified from Soong and Cotrufo (2015). We separated MAOC into a sand fraction and a siltclay fraction because they vary in turnover time, and the silt-clay fraction is considered more important in determining C stabilization (Poeplau et al., 2018). Therefore, from now on we will only consider the silt-clay fraction as MAOC. Size and density cutoffs were chosen based on conceptual work outlined in Lavallee et al. (2020). Briefly, 5g of oven-dried soil was dispersed in 1.65gcm⁻³ sodium polytungstate (SPT) by applying 200 Jml⁻¹ ultrasonic energy at 60 W. After centrifugation (2500g for 60min), the floating light fraction (representing POC) was aspirated and collected on a 0.45 µm glass fiber filter using a vacuum-filtration unit and rinsed with nanopure water. The heavy fraction pellet was washed with nanopure water and passed through a 53 µm sieve to separate the sand fraction (>53 μm) from the silt and clay fraction (<53 μm). All fractions were oven-dried (60°C), weighed and then finely ground. The ground fractions were analyzed for % C and % N on a Flash EA 1112 NC analyzer (Thermo Fisher Scientific Inc.). During sample processing we recovered $100\% \pm 1\%$ (mean \pm SD) of the soil mass, $108\% \pm 14\%$ of the C and $106\% \pm 17\%$ of the N.

2.7 | Carbon stabilization efficiency and CUE

We estimated CSE and CUE in the same incubation using the methods described by Geyer et al. (2020) and the following equations:

$$CSE = \frac{{}^{13}Soil C}{{}^{13}Soil C + {}^{13}CO_2},$$
 (1)

¹³Soil C = Soil C ×
$$\frac{\text{at \% } C_L - \text{at \% } C_{\text{ref}}}{\text{at \% label - at \% } C_{\text{ref}}},$$
 (2)

$$^{13}CO_{2} = cumulative \, ^{12}CO_{2} \times \frac{at \% \, C_{L} - at \% \, C_{ref}}{at \% \, label - at \% \, C_{ref}}, \tag{3}$$

where Soil C = the total C in soil samples (μ g Cg⁻¹ dry soil), at% C_L = the ¹³C at% of labelled soil (Equation 2) or CO₂ (Equation 3) samples, at% $C_{\rm ref}$ = the ¹³C at% of natural abundance control soil (Equation 2) or CO₂

(Equation 3) samples, at% label = the 13 C at% of the label solution (5 at%), and Cumulative 12 CO $_2$ = the cumulative CO $_2$ respired over the incubation period (μ g CO $_2$ -C g $^{-1}$ dry soil). Respiration data were blank-corrected using empty mason jars that were flushed with CO $_2$ -free air and incubated in parallel with soil samples. The cumulative 13 CO $_2$ produced during the 2-week incubation was estimated by first calculating hourly flux rates at four timepoints during the incubation (0-24h, 24–72h, 5-7 days, and 12–14 days), and then pairing each of the hourly flux rates with four distinct periods (0–1 days, 1–4 days, 4–8 days, and 8–14 days, respectively). We then estimated the cumulative 13 CO $_2$ produced by multiplying each hourly flux rate by the number of hours in each paired period and then adding the products. We used this approach to maximize sampling resolution during early stages of the incubation, since preliminary tests showed CO $_2$ flux rates were more variable at the start of the incubation (0–24h and 24–72h) than at the end (8–14 days).

Carbon use efficiency was estimated as:

$$CUE = \frac{^{13}Mic C}{^{13}Mic C + ^{13}CO_2},$$
 (4)

$$^{13}\text{Mic C} = (\text{Chl DOC} - \text{NChl DOC}) \times \frac{\text{at \% Mic } C_{\text{L}} - \text{at \% Mic } C_{\text{ref}}}{\text{at \% label} - \text{at \% Mic } C_{\text{ref}}}, \quad (5)$$

$$at\,\%\,Mic\,C = \frac{\left[(at\,\%\,Chl\,DOC \times Chl\,DOC) - (at\,\%\,NChl\,DOC \times NChl\,DOC) \right]}{(Chl\,DOC - NChl\,DOC)}, \tag{6}$$

where Chl DOC = the total C of $\rm K_2SO_4$ extracts fumigated with chloroform, NChl DOC = the total C of $\rm K_2SO_4$ extracts without chloroform, at% Chl = the at% of chloroform-fumigated extracts, at% NChl = the at% of non-chloroform-fumigated extracts, at% Mic $\rm C_L$ = the at% of microbial biomass in labelled samples, and at% Mic $\rm C_N$ = the at% of microbial biomass in natural abundance control samples. In some cases, $\rm ^{13}Mic$ C (Equation 5), and thus CUE, could not be calculated because NChl DOC was higher than Chl DOC (e.g., in the 2-week incubations at GRASS).

Since glucose is typically completely taken up by microbes within a few hours after it is added to soils, the ¹³C retained in soils in the CSE measurement represents ¹³C in microbial biomass and ¹³C in microbially-produced residues, thought to contribute to long-term soil C storage (Geyer et al., 2020). We measured CSE and CUE in both short- (24h) and long-term (2 weeks) incubations. The shortterm incubation is defined as the microbial community-scale CSE (CSE_c) and CUE (CUE_c), and is thought to closely track the efficiency of the microbial community to incorporate C in microbial products (Geyer et al., 2016). In contrast, the long-term incubation represents ecosystem-scale CSE (CSE_E) and CUE (CUE_E) and integrates microbial community-scale dynamics and the recycling of microbial necromass and residues, and is thus affected by soil organo-mineral interactions (Geyer et al., 2016). We chose 24h for short-term incubations as it is a widely used incubation time, facilitating comparisons with other studies. We chose 2 weeks for long-term incubations because preliminary tests showed that the CO₂ pulse after label addition was largely over after 2 weeks, and thus no significant further

TABLE 3 Soil extracellular enzymes measured and their abbreviations and functions

Enzyme	Abbreviation	Function
α-glucosidase	AG	Starch degradation; C acquisition
1,4-β-cellobiohydrolase	СВН	Cellulose degradation; C acquisition
β-glucosidase	BG	Cellulose degradation; C acquisition
N-acetyl-ß-D- glucosaminidase	NAG	Chitin degradation; N acquisition
L-Leucine aminopeptidase	LAP	Peptide breakdown; N acquisition
Phosphomonoesterase	PHO	Organic phosphorus degradation; P acquisition

partitioning of ¹³C between soil and atmosphere is expected after that point (Geyer et al., 2020).

We measured CSE and CUE exclusively on beneath shrub samples during the wet season when soils are moist to support microbial communities—summers at our site can extend >6 months without precipitation, representing a period of significantly decreased decomposition and microbial activity (Aronson et al., 2019; Schimel, 2018). Moreover, due to higher microbial densities, the microbial pump and effects of CSE and CUE are likely more important in soils beneath shrubs than in the interspaces (Sokol & Bradford, 2019). Detailed methods used to measure CSE and CUE are included in the Supporting Information.

2.8 | Statistical analyses

In CHAP and CSS1, we tested for significant N-fertilization treatment effects using three-way mixed ANOVAs with treatment and soil position (beneath shrub vs. interspace) as between-subject factors and season as within-subject factor. If a significant (p<.05) or marginally significant (p<.1) treatment effect was found, we used two-way ANOVAs to test for significant treatment effects within each season, using treatment and soil position as between-subject factors. If a significant (p<.05) or marginally significant (p<.1) treatment effect was found within either season, we used paired post-hoc t-tests to test for treatment effects within each soil position. P-values in the post-hoc tests were Bonferroni-corrected to account for an increase in type-1 error due to multiple comparisons. We checked for normal distribution of the tested variables using Shapiro-Wilk tests after standardizing and pooling data points from both treatments and microhabitats (beneath shrubs and in the



interspaces between shrubs). Variance homogeneity was evaluated by comparing standard deviations visually. If assumptions were not met, data were log-transformed, square root-transformed or multiplicative inverse-transformed, in that order. Since at GRASS and CSS2 we only took samples from beneath shrubs, we tested for significant N-fertilization treatment effects using two-way mixed ANOVAs with treatment as between-subject factor and season as within-subject factor. Post-hoc testing, assumption testing, and data transformations were done similarly as for CHAP and CSS1. Since assumptions could not be met for NO_3^- and NH_4^+ , three-way and twoway ANOVAs for these variables were performed on aligned rank transformed data (Wobbrock et al., 2011). We treated control and Nfertilized plots as dependent in the post-hoc tests due to the paired plot design at our sites. This allows us to account for landscape-scale variation in soil and plant properties, improving the statistical power at the low sample sizes typical for long-term ecosystem studies. We only tested for treatment effects within each site and not across sites, since each site differs in multiple factors such as fertilizer type, acidification, vegetation, and site. The data that support the findings of this study can be accessed from Püspök (2022).

We constructed a structural equation model (SEM) to test how different soil variables affected POC and MAOC. The variables were selected based on conceptual frameworks of SOM formation outlined in the introduction and partially illustrated in Figure 1. The SEM was constructed based on maximum-likelihood estimation using the lavaan package in R (Rossel, 2012). Code can be accessed from Püspök (2022). The data were pooled from all four sites and both seasons (n = 96). We tested for multivariate normality of the tested variables using Henze-Zirkler's test. Multivariate normality was still not fulfilled after transformations since soil pH followed a bimodal distribution. Therefore, we used robust standard errors of path coefficients and a Satorra-Bentler scaled maximum-likelihood estimation to account for a potential bias introduced by violating the multivariate normality assumption (Curran et al., 1996; Satorra & Bentler, 1994), using the "MLM" function in the lavaan package. Model fit was evaluated by model chi-squared statistics, confirmatory factor index, Tucker Lewis index, and root mean square error of approximation. All statistical analyses were performed in R-Studio version 4.1.2 (R Core Team).

3 | RESULTS

3.1 | Soil organic C fractions

Nitrogen fertilization had no effect on POC at our sites (Figure 2), but it decreased MAOC (Figure 3, p=.002) at the acidified CHAP site; MAOC decreased by 16% across both microhabitats (beneath shrubs and in the interspaces between shrubs) and seasons. This decrease in MAOC at CHAP appeared to be stronger in the wet season than in the dry season (Figure 3; $p_{\rm adj.}=.052$). In contrast to CHAP, N fertilization did not affect MAOC at the other sites, including the CSS1 site that had also been acidified by N fertilization.

3652486, 2023. 6, Downloaded from https://onlinelibrary.wiley.com/doi/10.1111/gcb.16563 by University Of California, Wiley Online Library on [04/07/2023]. See the Terms and Cond

ons) on Wiley Online Library for rules of use; OA articles are governed by the applicable Creative Commons License

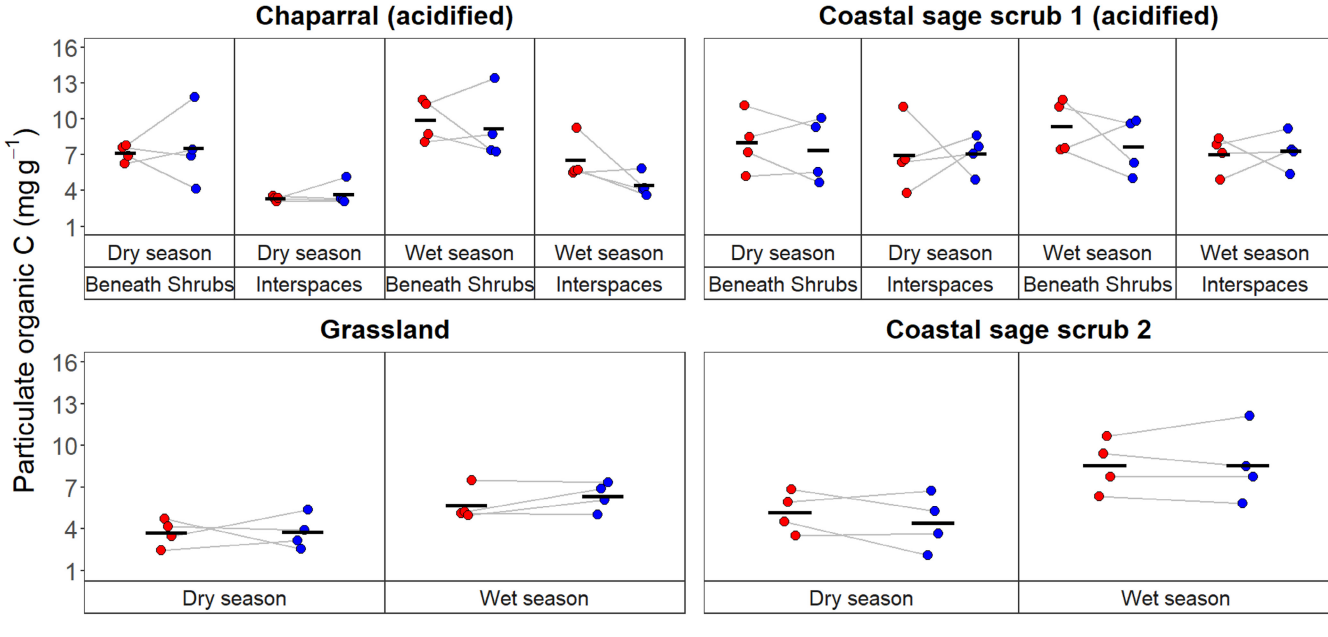


FIGURE 2 Differences in particulate organic C (POC) between control and N-fertilized plots during the dry season 2020 and the wet season 2021. At Chaparral and Coastal sage scrub 1, soils were sampled beneath shrubs and in interspaces between shrubs. At Grassland and Coastal sage scrub 2, soils were sampled beneath vegetation only. Chaparral and Coastal sage scrub 1 experienced strong acidification in response to N fertilization. Dots represent individual data points (four plots per treatment and soil position) with grey lines connecting paired control and N-fertilized plots. Black crossbars represent means (n = 4). No significant N fertilization effects (p < .1) were detected. [Colour figure can be viewed at wileyonlinelibrary.com]

Control
 N added

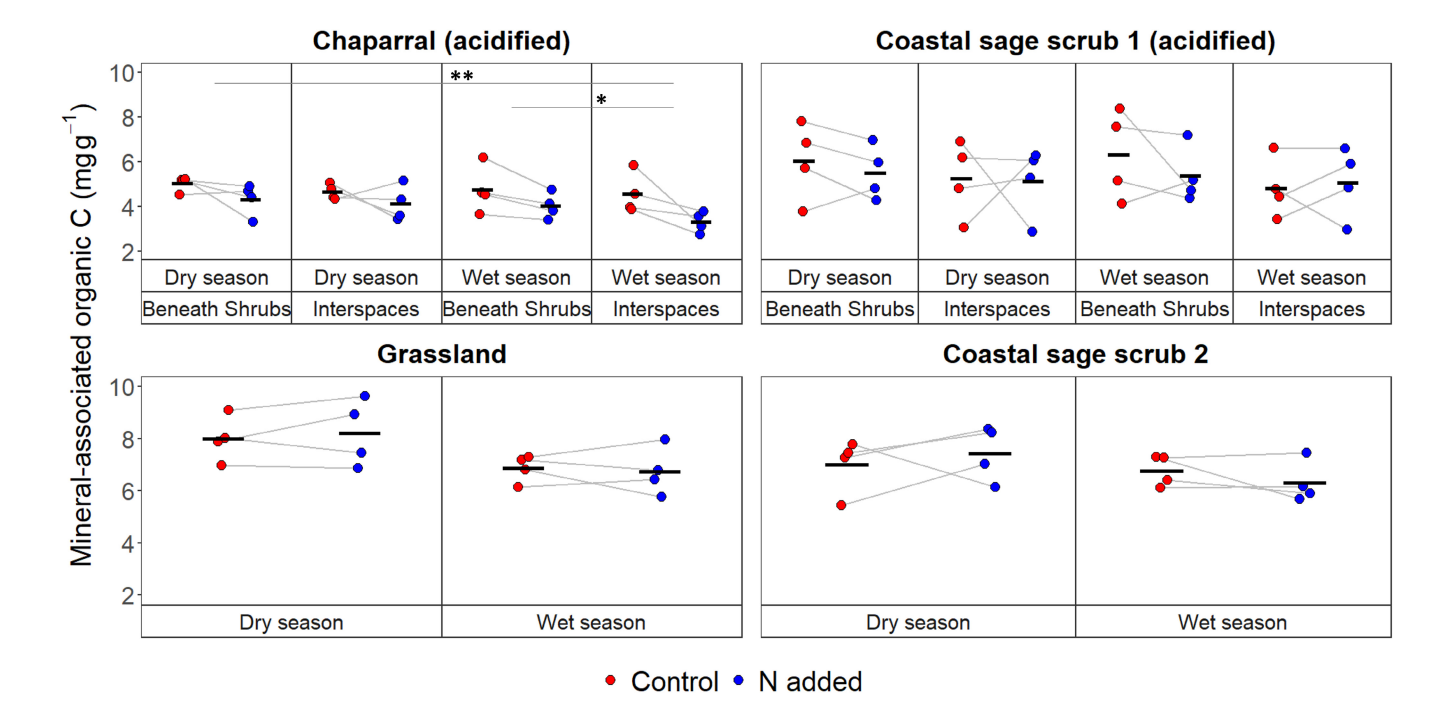


FIGURE 3 Differences in mineral-associated organic C between control and N-fertilized plots during the dry season 2020 and the wet season 2021. At Chaparral and Coastal sage scrub 1, soils were sampled beneath shrubs and in interspaces between shrubs. At Grassland and Coastal sage scrub 2, soils were sampled beneath vegetation only. Chaparral and Coastal sage scrub 1 experienced strong acidification in response to N fertilization. Dots represent individual data points (four plots per treatment and soil position) with grey lines connecting paired control and N-fertilized plots. Black crossbars represent means (n = 4). Significant N fertilization effects are indicated by black lines and asterisks directly above data points (*p < .1, **p < .05). [Colour figure can be viewed at wileyonlinelibrary.com]

3652486, 2023, 6, Downloaded from https://onlinelibrary.wiley.com/doi/10.1111/gcb.16563 by University Of California, Wiley Online Library on [04/07/2023]. See the Terms

ons) on Wiley Online Library for rules of use; OA articles are governed by the applicable Creative Commons I

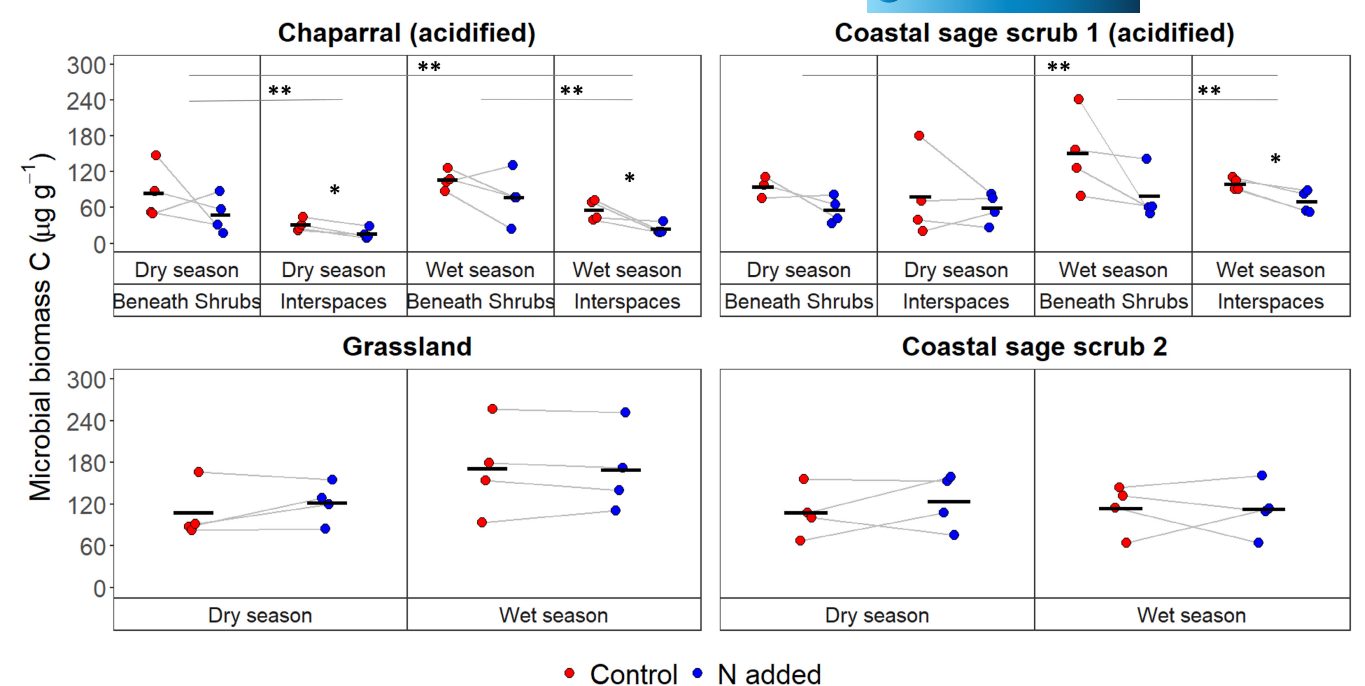


FIGURE 4 Differences in microbial biomass C between control and N-fertilized plots during the dry season 2020 and the wet season 2021. At Chaparral and Coastal sage scrub 1, soils were sampled beneath shrubs and in interspaces between shrubs. At Grassland and Coastal sage scrub 2, soils were sampled beneath vegetation only. Chaparral and Coastal sage scrub 1 experienced strong acidification in response to N fertilization. Dots represent individual data points (four plots per treatment and soil position) with grey lines connecting paired control and N-fertilized plots. Black crossbars represent means (n = 4). Significant N fertilization effects are indicated by black lines and asterisks directly above data points (*p < .1, **p < .05). [Colour figure can be viewed at wileyonlinelibrary.com]

3.2 | Microbial biomass and potential extracellular enzyme activities

N fertilization decreased microbial biomass C by 38% at the acidified CHAP site (Figure 4, p = .001) and by 24% at the acidified CSS1 site (Figure 4, p = .016), but had no effect on microbial biomass C at the other, unacidified, sites. At CHAP, N fertilization significantly decreased microbial biomass C in both the wet ($p_{\rm adj.}$ = .018) and the dry season ($p_{\rm adj.}$ = .048), with this effect trending to be mostly significant in the interspaces relative to beneath shrubs (Figure 4; $p_{\rm adj.}$ = .098 for wet season and $p_{\rm adj.}$ = .056 for dry season). At CSS1, N fertilization decreased microbial biomass C only in the wet season ($p_{\rm adj.}$ = .026) and only in the interspaces ($p_{\rm adj.}$ = .050).

Potential activities of all C- and N-acquiring extracellular enzymes decreased significantly with N fertilization at the acidified CHAP and CSS1 sites (Table 4), except for N-acquiring NAG which remained unchanged at CSS1. At CHAP, across both seasons and across microhabitats, AG decreased by 51% (p<.001), BG by 60% (p<.001), CBH by 47% (p<.001), NAG by 51% (p<.001), LAP by 62% (p<.001) and PHO by 57% (p<.001). At CSS1, AG decreased by 47% (p<.001), BG by 55% (p<.001), CBH by 48% (p<.001), LAP by 45% (p<.001) and PHO by 40% (p<.001). When we normalized enzyme activity on a per mg microbial biomass basis—to determine whether microbial investment in enzyme production changed—N fertilization did not affect enzyme activities at either site (Table S1), except for N-acquiring NAG which increased by 60% at CSS1 (p=.033). In contrast to the acidified sites,

N fertilization had no effect on potential soil extracellular enzyme activities at the non-acidified sites GRASS and CSS2 (Table 4).

3.3 | Carbon stabilization efficiency and CUE

Since we measured CSE and CUE only in soils sampled beneath shrubs during the wet season, we tested for an N fertilization effect on CSE and CUE with paired t-tests. Community-scale CSE (CSE_C), evaluated in the short-term incubations, decreased by $0.13\times$ in all eight N fertilization plots at CHAP and CSS1 relative to the control, but the difference was not significant at CHAP and only marginally significant at CSS1 (Figure 5, p=.095). In contrast to CSE_C, N fertilization had no effect on ecosystem-scale CSE (CSE_E) at CSS1, which was evaluated in long-term incubations (Figure 5). At CSS2, despite no changes in CSE_C, N fertilization marginally increased CSE_E by $0.14\times$ relative to controls (p=.073). No effects were detected at GRASS.

N fertilization significantly decreased community-scale CUE (CUE_C) by 0.45× at CHAP (Figure 6, p=.024) and by 0.25× at CSS1 (Figure 6, p=.006) relative to controls. N fertilization also decreased ecosystem-scale CUE (CUE_E) by 0.21× at CHAP (p=.027) relative to controls. Like CSE, at CSS2, N fertilization had no effect on CUE_C but marginally increased CUE_E by 0.32× relative to controls (p=.073). No effect was detected at GRASS, where only CUE_C could be calculated.

TABLE 4 Potential activities of C-acquiring soil extracellular enzymes alpha-glucosidase (AG), beta-glucosidase (BG) and cellobiohydrolase (CBH), N-acquiring soil extracellular enzymes Nacetyl-glucosaminidase (NAG) and leucine-aminopeptidase (LAP) and P-acquiring soil extracellular enzyme phosphomonoesterase (PHO)

	AG (nmolg ⁻¹ h ⁻¹)		CBH (nmolg ⁻¹ h ⁻¹) BG (nmolg ⁻¹ h ⁻¹)		¹)	NAG (nmol g ⁻¹ h ⁻¹)		LAP (nmol g ⁻¹ h ⁻¹)		PHO (nmol g ⁻¹ h ⁻¹)		
	Control	N added	Control	N added	Control	N added	Control	N added	Control	N added	Control	N added
Dry season (Octol	per 2020)											
CHAP												
Shrub	8.3 (0.6)	3.0 (0.9)	14.6 (5.0)	9.9 (8.6)	315.9 (79.5)	135.1 (98.7)	60.4 (14.7)	39.5 (24.9)	64.0 (7.1)	27.4 (8.5)	195.5 (29.5)	72.8 (27.0)
Interspace	3.4 (0.8)	1.9 (0.8)	4.0 (2.3)	2.0 (0.9)	94.7 (39.0)	39.6 (19.0)	25.0 (6.7)	12.5 (5.4)	50.2 (29.0)	19.8 (5.7)	130.1 (51.1)	64.1 (28.0)
CSS1												
Shrub	9.0 (0.9)	4.6 (1.1)	22.6 (8.5)	10.6 (3.1)	341.4 (109.2)	119.0 (29.1)	103.8 (30.6)	74.1 (14.4)	90.2 (13.7)	46.4 (6.4)	366.6 (59.8)	173.7 (44.4)
Interspace	9.8 (3.8)	6.0 (1.3)	15.4 (8.8)	11.6 (3.8)	218.7 (124.4)	154.5 (35.1)	94.2 (59.2)	82.1 (19.9)	89.8 (35.5)	61.6 (16.6)	349.6 (132.0)	221.0 (66.3)
GRASS	13.7 (1.6)	13.7 (1.6)	42.2 (19.9)	54.0 (11.1)	405.3 (123.1)	436.1 (107.0)	139.6 (45.2)	161.6 (28.4)	131.3 (31.6)	136.0 (32.0)	580.5 (141.8)	622.7 (107.3)
CSS2	9.2 (1.8)	9.5 (3.1)	23.8 (12.4)	30.5 (22.6)	232.8 (91.6)	268.2 (139.7)	72.3 (21.4)	93.1 (32.5)	78.6 (16.5)	92.7 (27.4)	414.4 (82.3)	476.9 (201.4)
Wet season (April	2021)											
CHAP												
Shrub	7.8 (1.6)	4.0 (1.3)	17.3 (8.7)	6.7 (2.3)	259.5 (118.9)	98.7 (24.6)	64.0 (26.9)	27.0 (9.4)	73.4 (20.5)	25.5 (3.8)	174.8 (80.7)	80.3 (25.6)
Interspace	4.7 (1.3)	3.0 (1.3)	4.7 (1.3)	3.0 (1.1)	81.1 (32.2)	25.4 (15.4)	29.7 (17.8)	9.2 (2.6)	41.2 (9.7)	13.8 (2.4)	116.7 (47.4)	49.3 (17.1)
CSS1												
Shrub	9.0 (1.2)	4.3 (1.6)	24.2 (7.0)	9.7 (3.8)	332 (162.7)	108.5 (30.3)	80.2 (18.4)	64.5 (8.9)	121.7 (23.2)	50.0 (21.0)	384.2 (106.2)	222.2 (59.5)
Interspace	6.5 (2.1)	3.4 (1.1)	9.8 (3.6)	5.3 (1.2)	123.2 (26.7)	75.2 (14.0)	46.9 (11.4)	70.0 (13.2)	73.4 (13.0)	48.9 (6.6)	237.4 (48.6)	189.6 (43.6)
GRASS	10.2 (1.4)	9.1 (1.8)	33.4 (8.5)	36.3 (12.6)	306.6 (35.8)	282.8 (73.4)	94.6 (6.3)	98.7 (16.7)	128.5 (5.8)	133.8 (24.1)	482.0 (78.1)	483.5 (143.8)
CSS2	8.4 (2.6)	7.0 (0.8)	20.3 (7.5)	18.2 (6.2)	204.0 (53.9)	162.3 (49.4)	57.9 (20.4)	62.7 (11.1)	99.8 (23.9)	102.7 (14.1)	391.0 (67.0)	394.6 (59.8)

Note: Data are means (standard deviation). Numbers in bold indicate significant differences between control and N-fertilized plots with N evaluated in a three-way mixed ANOVA across seasons and microhabitats for CHAP and CSS1 and in a two-way ANOVA across seasons for GRASS and CSS2 (p < .1).

3652486, 2023, 6, Downloaded from https://onlinelibrary.wiley.com/doi/10.1111/gcb.16563 by University Of California, Wiley Online Library on [04/07/2023]. See the Terms

of use; OA articles are governed by the applicable Creative Commons License

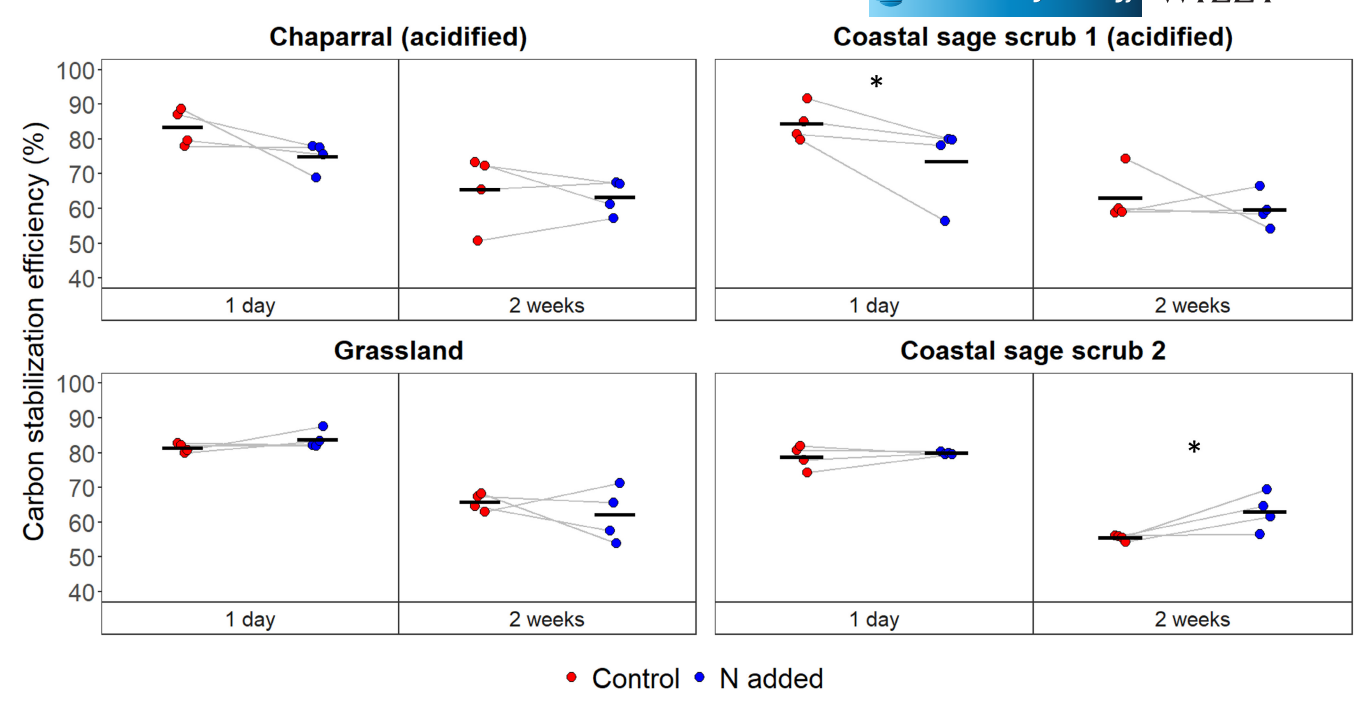


FIGURE 5 Differences in carbon stabilization efficiency measured in short- (1 day; i.e., community-scale carbon stabilization efficiency [CSE_C]) and long-term (2 weeks; i.e., ecosystem-scale carbon stabilization efficiency [CSE_E]) incubations between control and N-fertilized plots during the wet season 2021. Chaparral and Coastal sage scrub 1 experienced strong acidification in response to N fertilization. Dots represent individual data points (four plots per treatment and soil position) with grey lines connecting paired control and N-fertilized plots. Black crossbars represent means (n = 4). Significant N fertilization effects within each incubation time (paired t-test) are indicated by asterisks above data points (*p<.1, **p<.05). [Colour figure can be viewed at wileyonlinelibrary.com]

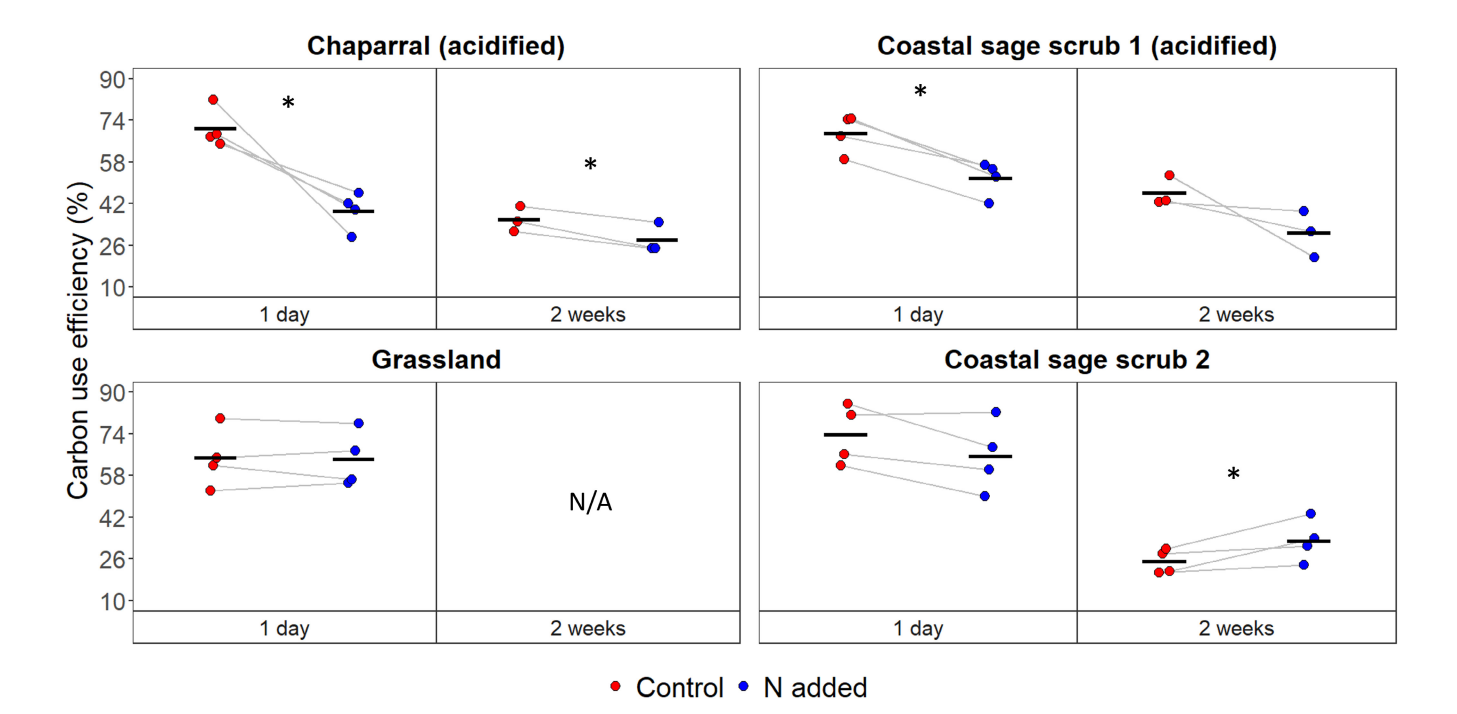


FIGURE 6 Differences in carbon use efficiency measured in short- (1 day; i.e., community-scale carbon use efficiency $[CUE_C]$) and long-term (2 weeks; i.e., ecosystem-scale carbon use efficiency $[CUE_E]$) incubations between control plots and plots fertilized with N during the wet season 2021. Chaparral and Coastal sage scrub 1 experienced strong acidification in response to N fertilization. Dots represent individual data points (four plots per treatment and soil position) with grey lines connecting paired control and N-fertilized plots. Black crossbars represent means (n = 4). For the 2-week incubation, one sample was lost for Chaparral and Coastal sage scrub 1 (n = 3) and Grassland has no data because CUE could not be calculated (see Section 2). Significant N fertilization effects within each incubation time (paired t-test) are indicated by asterisks above data points (*p < .1, **p < .05). [Colour figure can be viewed at wileyonlinelibrary.com]

3.4 | Soil exchangeable calcium

Long-term N fertilization had no effect on exchangeable Ca in nonacidified sites, but reduced soil exchangeable Ca at acidified sites (Figure 7); exchangeable Ca decreased by 47% at CHAP (p < .001) and by 16% at CSS1 (p = .003) when analyzed across season and across samples beneath shrubs and in the interspaces, albeit with a marginally significant interaction between treatment effect and soil position at CSS1 (p = .051). At CHAP, N fertilization significantly decreased exchangeable Ca in both the wet ($p_{adi.} = .007$) and the dry season ($p_{adi} = .003$). When analyzing the microhabitats individually, only beneath shrubs during the dry season samples decreased significantly with N fertilization ($p_{adi.} = .033$). At CSS1, N fertilization reduced exchangeable Ca in both seasons ($p_{adi} = .022$ for wet season and $p_{adi.} = .001$ for dry season). However, there was a significant interaction between the treatment and soil position in the dry season ($p_{adi} = .004$) where exchangeable Ca decreased only beneath shrubs (p_{adi} = .006). In the wet season, N fertilization significantly decreased exchangeable Ca only in interspaces ($p_{adi} = .038$).

3.5 | Controls over soil organic C fractions

The constructed SEM validated the importance of abiotic soil characteristics in driving variation in MAOC (Figure 8). Soil pH explained 33% of variation in exchangeable Ca across fertilization treatments,

sites, seasons, and microhabitats. Together with POC, soil pH and exchangeable Ca explained 45% of variation in microbial biomass. MAOC was strongly and positively affected by exchangeable Ca, which directly and, through its positive effect on microbial biomass, explained 58% of the variation in MAOC. In contrast, variation in POC was not well explained by our chosen soil variables—soil pH and exchangeable Ca only explained 4% of variation in POC—consistent with the fact that N fertilization had no effect at our sites (Figure 2).

4 | DISCUSSION

We studied changes in soil C fractions in four dryland sites in Southern California that span three dominant vegetation types and have been fertilized with N for more than 13 years. Two sites (CHAP and CSS1) were fertilized with urea, $\mathrm{NH_4}^+$, and $\mathrm{NO_3}^-$, and strongly acidified, whereas the other two sites (GRASS and CSS2) were fertilized with $\mathrm{CaNO_3}$ to prevent acidification. Fertilization had no effects on soil C fractions, except for at one site, where the MAOC fraction decreased likely because of changes in soil physicochemical properties induced by acidification. Contrary to previous studies, POC did not increase despite above-ground biomass increasing in three of the four study systems (Parolari et al., 2012; Vourlitis, Jaureguy, et al., 2021) coupled to a likely decrease in biotic decomposition in soil–soil microbial biomass and extracellular enzyme activities decreased—in the two sites that experienced strong acidification. Furthermore, we found

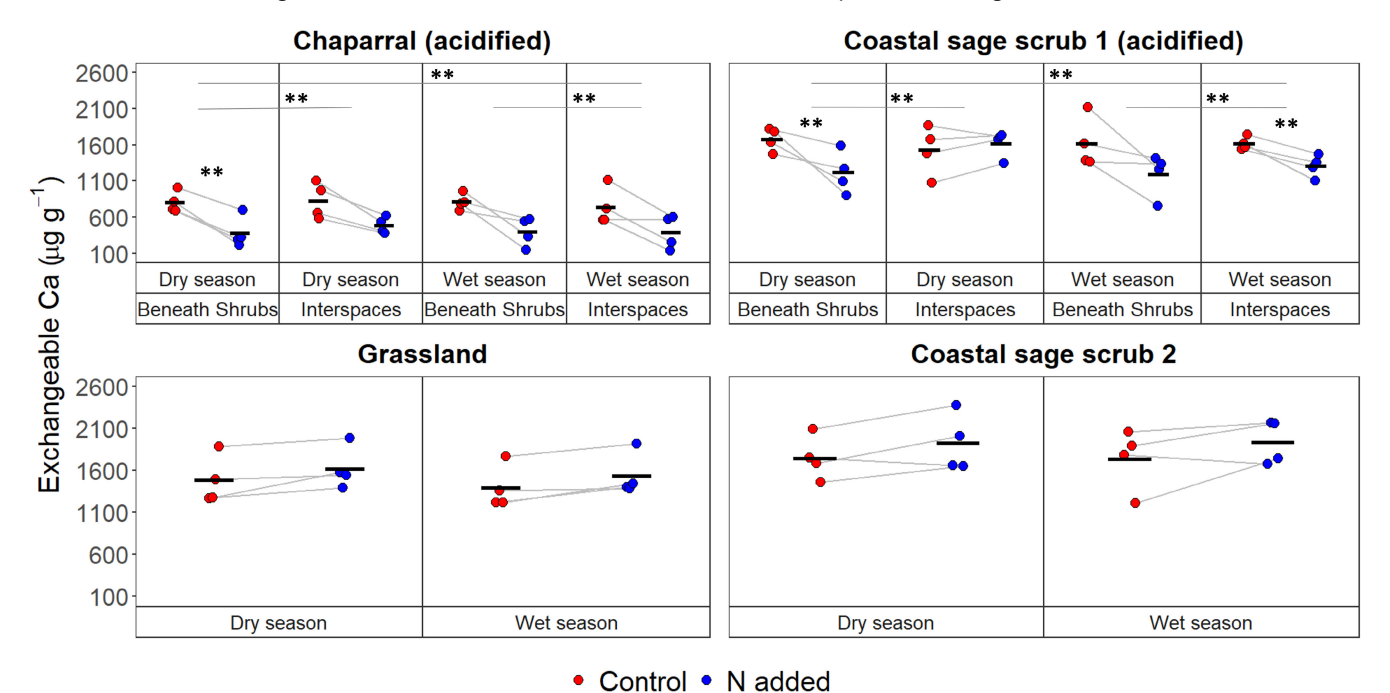


FIGURE 7 Differences in soil exchangeable Ca between control and N-fertilized plots during the dry season 2020 and the wet season 2021. At Chaparral and Coastal sage scrub 1, soils were sampled beneath shrubs and in interspaces between shrubs. At Grassland and Coastal sage scrub 2, soils were sampled beneath vegetation only. Chaparral and Coastal sage scrub 1 experienced strong acidification in response to N fertilization. Dots represent individual data points (four plots per treatment and soil position) with grey lines connecting paired control and N-fertilized plots. Black crossbars represent means (n = 4). Significant N fertilization effects are indicated by black lines and asterisks directly above data points (*p < .1, **p < .05). [Colour figure can be viewed at wileyonlinelibrary.com]

FIGURE 8 Structural equation model depicting how measured soil variables (n = 96) affect particulate organic C (POC) and mineral-associated organic C (MAOC) across control and N-fertilized plots during the dry season 2020 and the wet season 2021. Numbers next to boxes indicate the variation in the variable explained by the pathways leading to it. Numbers next to arrows indicate standardized path coefficients (robust standard errors of coefficients). Red lines indicate negative relationships and grey, dashed lines indicate non-significant pathways (p > .1). Thickness of arrows represent the relative importance of pathways. Model statistics: Robust $\chi^2 = 2.279$ (p = .131), robust comparative fit index (CFI) = 0.993, robust root mean square error of approximation (RMSEA) = 0.115. [Colour figure can be viewed at wileyonlinelibrary.com]

no evidence for a microbial C pump governing the persistence of soil C under N enrichment in these drylands; long-term but not short-term CUE and CSE increased in one of the non-acidified sites but did not lead to changes in MAOC. Importantly, however, we observed significant losses of MAOC at the acidified CHAP site, likely because of pH-induced Ca loss that destabilized organo-mineral interactions. Our measurements suggest that long-term effects of N fertilization on dryland C storage are of abiotic nature, such that drylands where Ca-stabilization of SOC is prevalent may be most at risk for significant MAOC losses.

4.1 | POC dynamics

We hypothesized N fertilization would increase POC due to increased plant biomass production as observed in semi-arid grasslands in China (Ye et al., 2018) and Mediterranean grasslands in California (Lin et al., 2019). However, despite N fertilization increasing above-ground plant biomass at CHAP, CSS1, and GRASS (data for CSS2 are not available) (Parolari et al., 2012; Vourlitis, Jaureguy, et al., 2021), POC did not increase. It is possible that N fertilization could have increased microbial respiration of plant C inputs, preventing POC accumulation in soils (Finn et al., 2015; Khan et al., 2007; Knorr et al., 2005), but this is unlikely at our sites. This is because although adding N increased litter quality at GRASS (Allison

et al., 2013), neither litter decomposition rates (Allison et al., 2013) nor soil microbial respiration rates increased (measured in CUE incubations; Figure S1). Furthermore, N fertilization is predicted to stimulate microbial decomposition only if pH remains relatively constant (Averill & Waring, 2018), but CHAP and CSS1 experienced strong acidification, decreasing both soil microbial biomass and hydrolytic soil extracellular enzymes—putative proxies signaling high potential for organic matter decomposition. Indeed, soil microbial respiration rates (measured in CUE incubations only in wet season and only beneath shrubs) decreased by 61% in fertilized plots at CHAP (p = .088) and not significantly in CSS1 (Figure S1). This is in line with findings from semi-arid grasslands in China, where N fertilization led to soil acidification together with decreases in microbial biomass and soil respiration (Chen et al., 2016). While no data on litter decomposition rates exist, the strong decrease in soil microbial biomass and almost all potential soil hydrolytic enzyme activities, suggests that microbial soil organic matter decomposition was suppressed in acidified sites, which in other studies has typically increased POC (Treseder, 2008; Zak et al., 2019). Therefore, other processes are likely preventing POC from building up in these drylands.

The fact that increased aboveground biomass production did not lead to increases in POC could mean that roots are more important for building POC at our sites. It is well established that aboveground litter in drylands can degrade photochemically before being incorporated in the soil, independent of litter and soil properties (Austin

& Vivanco, 2006). In some dryland soils this suggests aboveground litter contributes little to soil organic C, and that root biomass contributes most to POC (e.g., Berenstecher et al., 2021). Therefore, the response of POC to N deposition may depend more on changes in root production. Indeed, a fertilization study in a semi-arid grassland found POC increased together with root biomass (Ye et al., 2018). While root data is not available for GRASS and CSS2, cumulative root production was unchanged after the first 15 years of fertilization at CHAP and CSS1 (Vourlitis, Jaureguy, et al., 2021), potentially explaining why POC did not change despite increases in aboveground biomass. Overall, our data suggest that increased above-ground biomass production is decoupled from POC at our sites, and that POC may be more affected by root production.

In addition to aboveground decomposition, POC may have not increased at our sites because the effects of N fertilization may be confounded by annual changes in plant biomass production and decomposition in response to precipitation. Precipitation strongly affects plant biomass production and its response to N fertilization in drylands (Hou et al., 2021; Yahdjian et al., 2011), with several studies showing N fertilization increased plant production only under experimental water addition (Ma et al., 2020) or in years with above-average precipitation (Hall et al., 2011; Ladwig et al., 2012; Su et al., 2013; Vourlitis, 2012). Similarly, dryland soils can experience high seasonal and year-to-year variation in SOC (Hou et al., 2021). The strong seasonal changes we observed in POC from the dry to the wet season (+47% for POC and only -5% for MAOC, Figure 2 and Figure 3) suggest that much of the seasonal variation in SOC (+13% in our study, Table 2) observed in drylands is driven by changes in POC, which is considered a more dynamic pool than MAOC (Lavallee et al., 2020). Furthermore, wind, water, and faunal activity can horizontally and vertically transport litter and POC from where it has been produced (Throop & Belnap, 2019). Therefore, seasonal changes might make it challenging to detect differences in POC and, by extension, in SOC. For example, SOC at CHAP and CSS1 responded negatively, positively, or not at all to N fertilization depending on the year of measurement (Vourlitis, Kirby, et al., 2021), while another study found increases in SOC at CSS2 in 2012 where we found no changes (Khalili et al., 2016). Overall, even if differences in POC may have been detected in some years, the observed dynamic nature of POC suggests that much of the POC in our study may turn over relatively fast, with only a small fraction contributing to long-term C storage.

4.2 Microbial C use and stabilization efficiency

We found limited evidence (i.e., changes in CSE or MAOC) for an acceleration of the microbial C pump under N fertilization in the non-acidified sites at GRASS and CSS2. It has been suggested that if soils have a high enough sorption potential and do not acidify, N fertilization should alleviate microbial N limitation, increasing microbial CUE and, thereby, MAOC (Averill & Waring, 2018; Manzoni et al., 2012; Poeplau et al., 2019). While we found no changes in

short-term CUE or CSE at GRASS or CSS2, long-term CUE and CSE increased at CSS2, but without increasing MAOC. Short-term CUE and CSE are mostly regulated by microbial community physiological responses, whereas long-term incubations also include effects of organo-mineral interactions and recycling of C exudates (Geyer et al., 2016). The lack of a response to N fertilization in short-term incubations could indicate that, in drylands, microbes may be instead mostly limited by water and C availability (Homyak et al., 2018; Schaeffer et al., 2003; Schimel, 2018). Alternatively, microbial CUE can also change in response to changes in microbial community composition (Li et al., 2021). While microbial community composition changed at GRASS (Amend et al., 2016), the changes may not have been directed enough to favor microbes with a higher CSE (Pold et al., 2020). Thus, the increase in long-term, but not short-term CUE and CSE in fertilized plots at CSS2 suggests more efficient recycling of C compounds (Geyer et al., 2016), which after more than ten years of N fertilization has not led to detectable changes in MAOC. Overall, N fertilization did not increase dryland C storage through changes in microbial CUE or CSE.

It is possible we did not detect an acceleration of the microbial C pump under N fertilization because the low sorption potential of soils at our sites inhibits the microbial in-vivo pathway of C stabilization (Islam et al., 2022; Liang et al., 2017). For example, short-term CSE decreased in all N deposition plots at CHAP and CSS1 but had no effect on long-term CSE. The fact that short- and long-term CUE decreased in all N deposition plots at CHAP and CSS1 suggests that microbial community changes and microbial stress in response to acidification could have accounted for the decrease in short-term CSE at CHAP and CSS1 (Grant et al., 2022; Jones et al., 2019; Lauber et al., 2009). However, the fact that the initial differences in CSE did not translate into long-term stabilization means that the additional C that was initially retained in control plots was later recycled and respired over the course of the long-term incubation (Geyer et al., 2016, 2020). Similar to a previous study on low-sorption sandy soils (Creamer et al., 2014), this could indicate that the C stabilization potential in the studied soils is too low, so that even if microbes initially retain C more efficiently, there is no viable mechanism for long-term storage (Islam et al., 2022)—the soils may be operating at or near their capacity to store C. Therefore, it is unlikely that N addition would affect C stabilization at our site via the microbial C pump, as microbial C accumulation efficiency may strongly depend on soil mineralogy (Cai et al., 2022).

4.3 | Changes in MAOC

We found significant MAOC losses in response to N fertilization at CHAP; N fertilization lowered MAOC by 13% in the dry season and by 21% in the wet season relative to control plots (Figure 3). MAOC losses in drylands have been observed before and linked to increased decomposition related to changes in microbial physiology (Lin et al., 2019) and/or acidification (Ye et al., 2018). However, an increase in MAOC decomposition rates at our site

Global Change Biology -WILEY

due to changes in microbial physiology is unlikely since biotic decomposition likely decreased at CHAP as we discussed earlier for POC. Furthermore, the fact that the decrease in MAOC was also observed in the interspaces between shrubs, where we found significantly lower microbial biomass, points to acidification as the likely driver behind the MAOC decrease, not changes in microbial physiology.

Acidification can decrease MAOC by destabilizing Ca-organic C associations that make the C accessible to microbes or vulnerable to loss via dissolved organic C (Bailey et al., 2019). Polyvalent cations such as Ca are important in bridging negatively charged C compounds to negatively charged mineral surfaces, particularly in dryland soils (Rasmussen et al., 2018; Rowley et al., 2018). Even though we did not measure Ca-organic C pools directly, exchangeable Ca was strongly correlated with MAOC and significantly decreased at CHAP (Figure 6), suggesting that Ca loss is the main pathway for MAOC loss at our sites. This is consistent with results from nine temperate grasslands across the United States where soil texture and mineralogy were key predictors of SOC more so than N fertilization (Keller et al., 2022), suggesting that N-induced acidification can directly affect soil physical factors that control MAOC. This mechanism was further supported by our SEM, highlighting that MAOC was correlated with exchangeable Ca, which both directly, and indirectly through microbial biomass, explained 58% of the variation in MAOC (Figure 8). Our findings are also consistent with studies in mesic agricultural systems (Wan et al., 2021) and semi-arid grasslands in China (Ye et al., 2018) reporting losses in Ca-associated organic matter in response to N-induced acidification, suggesting MAOC loss was primarily related to pH-induced destabilization of Ca-organic C associations.

While a loss of Ca-associated organic matter can explain the loss of MAOC at our CHAP site, we found that strong acidification and loss of exchangeable Ca did not decrease MAOC at CSS1. On average the finer-textured (see Table S2 for texture) CSS1 lost less Ca than the coarser-textured CHAP (16% vs. 47%) and had higher baseline Ca levels (1.6 mg g⁻¹ at CSS1 averaged across microhabitats and seasons in control plots vs. $0.8 \,\mathrm{mg\,g^{-1}}$ at CHAP), perhaps suggesting that there is a threshold beyond which decreases in exchangeable Ca destabilize cation bridges and Ca-associated organic matter. However, we found that out of the sixteen studied N addition cases at CSS1 (4 plots × 2 seasons × 2 microhabitats), six did not decrease in MAOC. Four of these six cases come from two plots at CSS1 which experienced significant dieback of native shrub vegetation and replacement by invasive forbs (George Vourlitis, personal communication). It is possible that a change to a faster cycling grass- and forb-dominated vegetation system with higher root biomass and turnover overrode potential Ca-related C losses and led to C accumulation in these plots (Qi et al., 2019); strong increases in SOC upon CSS invasion by grasses have been observed before (Wolkovich et al., 2010). Since N enrichment is expected to shift plant community composition (Plaza, Gascó, et al., 2018), particularly in CSS (Kimball et al., 2014; Valliere et al., 2017), future studies on how effects of vegetation change

on SOC fractions might interact with direct effects of N addition are warranted.

4.4 | Implications for N deposition effects on C storage in drylands

Given the high seasonal fluctuation in SOC and POC in drylands (this study; Hou et al. 2021; Vourlitis, Kirby, et al., 2021), the consistently observed MAOC losses at CHAP could be the first sign for a future decrease in C storage in soils prone to acidification. Notably, even more alkaline soils considered to be better buffered against pH changes than soils in our study can acidify over time (Tian & Niu, 2015; Yang et al., 2012). If acidification occurs, Ca leaching and concurrent C losses may be mostly restricted to topsoils in areas in which Caassociations make up an important fraction of C stabilization (Niu et al., 2021), although data are limited. While there is currently no good understanding of the distribution of Ca-associated organic C pools, correlation studies suggest that Ca is particularly important for C stabilization in drylands above pH 6.5 and dominated by 2:1 phyllosilicates (Rasmussen et al., 2018). Potential decreases in topsoil C in these areas could have important consequences for soil structure, water holding capacity, and soil fertility. Notably, inputs of aboveground biomass might not help to balance these losses if aboveground litter does not build up in soils as we and others observed (Berenstecher et al., 2021), particularly since root biomass does not always increase in response to N enrichment (Kummerow et al., 1982; Ladwig et al., 2012; Vourlitis, Jaureguy, et al., 2021; Zeng et al., 2010). Furthermore, the form of N deposited, either as NH₄⁺ or NO₃⁻, can affect soil acidification (Tian & Niu, 2015). While NH3 emission can initially buffer acidity in precipitation, once deposited, NH₄⁺ can still cause acidification depending on whether it is taken up by plants or nitrified (Rodhe et al., 2002). Nitrification produces 2 H+ ions and NO_3^- , and the NO_3^- can then co-leach as a companion anion to base cations enriching sites with H⁺ (Rodhe et al., 2002). Since a global shift from NO₃⁻ to NH₃ deposition is expected (Kanakidou et al., 2016; Lamarque et al., 2013), future studies should focus specifically on how the deposition and consumption pathways of these compounds affect acidification and C dynamics in drylands.

5 | CONCLUSION

We sampled soils at four long-term N-fertilization sites in Southern California to understand how increasing rates of atmospheric N deposition may affect SOC dynamics in drylands. In contrast to studies from forest soils where N enrichment decreases microbial biomass, extracellular enzyme activity, and respiration with a concomitant increase in SOC (Janssens et al., 2010; O'Sullivan et al., 2019; Riggs & Hobbie, 2016; Treseder, 2008), we found that N enrichment had relatively small effects on SOC storage, with no C accumulating in these dryland soils despite non-acidic conditions that were expected to build SOC via the microbial C pump (Averill & Waring, 2018; Liang

et al., 2017). However, in soils experiencing strong N-induced acidification, we observed substantial Ca losses that destabilized MAOC in one of the sites. As soils saturate with N (Homyak et al., 2014), our measurements highlight a pH-dependent mechanism whereby Ca-stabilization of SOC in drylands may decrease, leading to a loss of SOC. Overall, microbial processes in dryland soils may be ultimately governed by C and water availability, suggesting that N enrichment is unlikely to benefit SOC, and instead favor decreases in SOC as a result of decalcification of the soil and destabilization of MAOC.

ACKNOWLEDGMENTS

We thank reserve managers at Santa Margarita and Sky Oaks ecological reserves, and the Irvine Ranch Conservancy and Orange County Parks for access to research sites. We thank Dr. Kevin Geyer for assistance with the CUE method and Dr. Gabriela Mendoza for artwork design. This research was supported by the United States National Science Foundation (award DEB 1916622 to P.M.H., E.J.H., E.L.A., and J.P.S.) and the US Department of Energy, Office of Science, BER award DE-SC0020382 to S.D.A.

CONFLICT OF INTEREST

The authors declare no conflict of interest.

DATA AVAILABILITY STATEMENT

Data can be accessed at: http://doi.org/10.17605/OSF.IO/W78VD.

ORCID

Johann F. Püspök https://orcid.org/0000-0001-6946-1030 Sharon Zhao https://orcid.org/0000-0001-5844-7575 George L. Vourlitis https://orcid.org/0000-0003-4304-3951 Steven D. Allison https://orcid.org/0000-0003-4629-7842 Emma L. Aronson https://orcid.org/0000-0002-5018-2688 Joshua P. Schimel https://orcid.org/0000-0002-1022-6623 Erin J. Hanan https://orcid.org/0000-0001-6568-2936 Peter M. Homyak https://orcid.org/0000-0003-0671-8358

REFERENCES

- Allison, S. D., Lu, Y., Weihe, C., Goulden, M. L., Martiny, A. C., Treseder, K. K., & Martiny, J. B. H. (2013). Microbial abundance and composition influence litter decomposition response to environmental change. *Ecology*, *94*, 714–725. https://doi.org/10.1890/12-1243.1
- Amend, A. S., Martiny, A. C., Allison, S. D., Berlemont, R., Goulden, M. L., Lu, Y., Treseder, K. K., Weihe, C., & Martiny, J. B. H. (2016). Microbial response to simulated global change is phylogenetically conserved and linked with functional potential. *ISME Journal*, 10, 109–118. https://doi.org/10.1038/ismej.2015.96
- Aronson, E. L., Goulden, M. L., & Allison, S. D. (2019). Greenhouse gas fluxes under drought and nitrogen addition in a Southern California grassland. *Soil Biology and Biochemistry*, 131, 19–27. https://doi.org/10.1016/j.soilbio.2018.12.010
- Austin, A. T., & Vivanco, L. (2006). Plant litter decomposition in a semiarid ecosystem controlled by photodegradation. *Nature*, 442, 555– 558. https://doi.org/10.1038/nature05038
- Averill, C., & Waring, B. (2018). Nitrogen limitation of decomposition and decay: How can it occur? *Global Change Biology*, 24, 1417–1427. https://doi.org/10.1111/gcb.13980

- Bailey, V. L., Pries, C. H., & Lajtha, K. (2019). What do we know about soil carbon destabilization? *Environmental Research Letters*, 14, 083004.
- Barbour, K. M., Weihe, C., Allison, S. D., & Martiny, J. B. H. (2022). Bacterial community response to environmental change varies with depth in the surface soil. Soil Biology and Biochemistry, 172, 108761. https://doi.org/10.1016/j.soilbio.2022.108761
- Berenstecher, P., Araujo, P. I., & Austin, A. T. (2021). Worlds apart: Location above- or below-ground determines plant litter decomposition in a semi-arid Patagonian steppe. *Journal of Ecology*, 109, 2885–2896. https://doi.org/10.1111/1365-2745.13688
- Bradford, M. A., Keiser, A. D., Davies, C. A., Mersmann, C. A., & Strickland, M. S. (2013). Empirical evidence that soil carbon formation from plant inputs is positively related to microbial growth. *Biogeochemistry*, 113, 271–281. https://doi.org/10.1007/s10533-012-9822-0
- Brookes, P. C., Landman, A., Pruden, G., & Jenkinson, D. S. (1985). Chloroform fumigation and the release of soil nitrogen: A rapid direct extraction method to measure microbial biomass nitrogen in soil. *Soil Biology and Biochemistry*, 17(6), 837-842. https://doi.org/10.1159/000477898
- Burns, R. G., DeForest, J. L., Marxsen, J., Sinsabaugh, R. L., Stromberger, M. E., Wallenstein, M. D., Weintruab, M. N., & Zoppini, A. (2013). Soil enzymes in a changing environment: Current knowledge and future directions. Soil Biology and Biochemistry, 58, 216–234. https://doi.org/10.1016/j.soilbio.2012.11.009
- Butcher, K. R., Nasto, M. K., Norton, J. M., & Stark, J. M. (2020). Physical mechanisms for soil moisture effects on microbial carbon-use efficiency in a sandy loam soil in the western United States. Soil Biology and Biochemistry, 150, 107969. https://doi.org/10.1016/j. soilbio.2020.107969
- Cai, Y., Ma, T., Wang, Y., Jia, J., Jia, Y., Liang, C., & Feng, X. (2022). Assessing the accumulation efficiency of various microbial carbon components in soils of different minerals. *Geoderma*, 407, 115562. https://doi.org/10.1016/j.geoderma.2021.115562
- Castellano, M. J., Mueller, K. E., Olk, D. C., Sawyer, J. E., & Six, J. (2015). Integrating plant litter quality, soil organic matter stabilization, and the carbon saturation concept. *Global Change Biology*, *21*, 3200–3209. https://doi.org/10.1111/gcb.12982
- Chen, D., Li, J., Lan, Z., Hu, S., & Bai, Y. (2016). Soil acidification exerts a greater control on soil respiration than soil nitrogen availability in grasslands subjected to long-term nitrogen enrichment. *Functional Ecology*, 30, 658–669. https://doi.org/10.1111/1365-2435.12525
- Cotrufo, M. F., Ranalli, M. G., Haddix, M. L., Six, J., & Lugato, E. (2019). Soil carbon storage informed by particulate and mineral-associated organic matter. *Nature Geoscience*, 12, 989–994. https://doi.org/10.1038/s41561-019-0484-6
- Creamer, C. A., Jones, D. L., Baldock, J. A., & Farrell, M. (2014). Stoichiometric controls upon low molecular weight carbon decomposition. *Soil Biology and Biochemistry*, 79, 50–56. https://doi.org/10.1016/j.soilbio.2014.08.019
- Creamer, C. A., Jones, D. L., Baldock, J. A., Rui, Y., Murphy, D. V., Hoyle, F. C., & Farrell, M. (2016). Is the fate of glucose-derived carbon more strongly driven by nutrient availability, soil texture, or microbial biomass size? *Soil Biology and Biochemistry*, 103, 201–212. https://doi.org/10.1016/j.soilbio.2016.08.025
- Curran, P. J., West, S. G., & Finch, J. F. (1996). The robustness of test statistics to nonnormality and specification error in confirmatory factor analysis. *Psychological Methods*, 1, 16–29.
- Deng, L., Huang, C., Shangguan, D. K. Z., Wang, K., Song, X., & Peng, C. (2020). Soil GHG fluxes are altered by N deposition: New data indicate lower N stimulation of the $\rm N_2O$ flux and greater stimulation of the calculated C pools. *Global Change Biology*, 26, 2613–2629. https://doi.org/10.1111/gcb.14970
- Fenn, M. E., Allen, E. B., Weiss, S. B., Jovan, S., Geiser, L. H., Tonnesen, G. S., Johnson, R. F., Rao, L. E., Gimeno, B. S., Yuan, F., Meixner, T., & Bytnerowicz, A. (2010). Nitrogen critical loads and management

- alternatives for N-impacted ecosystems in California. *Journal of Environmental Management*, 91, 2404–2423. https://doi.org/10.1016/j.jenvman.2010.07.034
- Fierer, N. (2003). Stress ecology and the dynamics of microbial communities and processes in soil. ProQuest Dissertations.
- Finn, D., Page, K., Catton, K., Strounina, E., Kienzle, M., Robertson, F., Armstrong, R., & Dalal, R. (2015). Effect of added nitrogen on plant litter decomposition depends on initial soil carbon and nitrogen stoichiometry. Soil Biology and Biochemistry, 91, 160–168. https://doi.org/10.1016/j.soilbio.2015.09.001
- Geyer, K., Schnecker, J., Grandy, A. S., Richter, A., & Frey, S. (2020). Assessing microbial residues in soil as a potential carbon sink and moderator of carbon use efficiency. *Biogeochemistry*, 4, 237–249. https://doi.org/10.1007/s10533-020-00720-4
- Geyer, K. M., Kyker-snowman, E., Grandy, A. S., & Frey, S. D. (2016). Microbial carbon use efficiency: Accounting for population, community, and ecosystem-scale controls over the fate of metabolized organic matter. *Biogeochemistry*, 127, 173–188. https://doi.org/10.1007/s10533-016-0191-y
- Grant, T., Sethuraman, A., Escobar, M. A., & Vourlitis, G. L. (2022). Chronic dry nitrogen inputs alter soil microbial community composition in Southern California semi-arid shrublands. Applied Soil Ecology, 176, 104496. https://doi.org/10.1016/j.apsoil.2022.104496
- Gruber, N., & Galloway, J. N. (2008). An Earth-system perspective of the global nitrogen cycle. *Nature*, 451, 293–296. https://doi.org/10.1038/nature06592
- Hall, S. J., Sponseller, R. A., Grimm, N. B., Huber, D., Kaye, J. P., Clark, C., & Collins, S. L. (2011). Ecosystem response to nutrient enrichment across an urban airshed in the Sonoran Desert. *Ecological Applications*, 21, 640–660. https://doi.org/10.1890/10-0758.1
- Hendershot, W. H., & Duquette, M. (1986). A simple barium chloride method for determining cation exchange capacity and exchangeable cations. Soil Science Society of America Journal, 50(3), 605–608. https://doi.org/10.2136/sssaj1986.03615995005000030013x
- Homyak, P. M., Blankinship, J. C., Slessarev, E. W., Schaeffer, S. M., Manzoni, S., & Schimel, J. P. (2018). Effects of altered dry season length and plant inputs on soluble soil carbon. *Ecology*, 99, 2348– 2362. https://doi.org/10.1002/ecy.2473
- Homyak, P. M., Sickman, J. O., Miller, A. E., Melack, J. M., Meixner, T., & Schimel, J. P. (2014). Assessing nitrogen-saturation in a seasonally dry chaparral watershed: Limitations of traditional indicators of N-saturation. *Ecosystems*, 17, 1286–1305. https://doi.org/10.1007/s10021-014-9792-2
- Hou, E., Rudgers, J. A., Collins, S. L., Litvak, M. E., White, C. S., Moore, D. I., & Luo, Y. (2021). Sensitivity of soil organic matter to climate and fire in a desert grassland. *Biogeochemistry*, 156, 59–74. https://doi.org/10.1007/s10533-020-00713-3
- Islam, M. R., Singh, B., & Dijkstra, F. A. (2022). Stabilisation of soil organic matter: Interactions between clay and microbes. *Biogeochemistry*, 160, 145–158. https://doi.org/10.1007/s10533-022-00956-2
- Janssens, I. A., Dieleman, W., Luyssaert, S., Subke, J., Reichstein, M., Ceulemans, R., Ciais, P., Dolman, A. J., Grace, J., Matteucci, G., Papale, D., Piao, S. L., Schulze, E.-D., Tang, J., & Law, B. E. (2010). Reduction of forest soil respiration in response to nitrogen deposition. *Nature Geoscience*, 3, 315–322. https://doi.org/10.1038/ngeo844
- Jones, D. L., Cooledge, E. C., Hoyle, F. C., Griffiths, R. I., & Murphy, D. V. (2019). pH and exchangeable aluminum are major regulators of microbial energy flow and carbon use efficiency in soil microbial communities. Soil Biology and Biochemistry, 138, 107584. https://doi.org/10.1016/j.soilbio.2019.107584
- Kanakidou, M., Myriokefalitakis, S., Daskalakis, N., Fanourgakis, G., Nenes, A., Baker, A. R., Tsigaridis, K., & Mihalopoulos, N. (2016). Past, present, and future atmospheric nitrogen deposition.

- Journal of the Atmospheric Sciences, 73, 2039–2047. https://doi.org/10.1175/JAS-D-15-0278.1
- Keller, A. B., Borer, E. T., Collins, S. L., DeLancey, L. C., Fay, P. A., Hofmockel, K. S., Leakey, A. D. B., Mayes, M. A., Seabloom, E. W., Walter, C. A., Wang, Y., Zhao, Q., & Hobbie, S. E. (2022). Soil carbon stocks in temperate grasslands differ strongly across sites but are insensitive to decade-long fertilization. *Global Change Biology*, 28(4), 1659–1677. https://doi.org/10.1111/gcb.15988
- Khalili, B., Ogunseitan, O. A., Goulden, M. L., & Allison, S. D. (2016). Interactive effects of precipitation manipulation and nitrogen addition on soil properties in California grassland and shrubland. Applied Soil Ecology, 107, 144–153. https://doi.org/10.1016/j. apsoil.2016.05.018
- Khan, S. A., Mulvaney, R. L., Ellsworth, T. R., & Boast, C. W. (2007). The myth of nitrogen fertilization for soil carbon sequestration. *Journal* of Environmental Quality, 36, 1821–1832. https://doi.org/10.2134/ jeq2007.0099
- Kimball, S., Goulden, M. L., Suding, K. N., & Parker, S. (2014). Altered water and nitrogen input shifts succession in a southern California coastal sage community. *Ecological Applications*, 24, 1390–1404. https://doi.org/10.1890/13-1313.1
- Knorr, M., Frey, S. D., & Curtis, P. S. (2005). Nitrogen additions and litter decomposition: A meta-analysis. *Ecology*, 86(12), 3252–3257. https://doi.org/10.1890/05-0150
- Kummerow, J., Avila, G., Aljaro, M.-E., Araya, S., & Montenegro, G. (1982).
 Effect of fertilizer on fine root density and shoot growth in Chilean matorral. *Botanical Gazette*, 143, 498–504.
- Ladwig, L. M., Collins, S. L., Swann, A. L., Xia, Y., Allen, M. F., & Allen, E. B. (2012). Above- and belowground responses to nitrogen addition in a Chihuahuan Desert grassland. *Oecologia*, 169, 177–185. https://doi.org/10.1007/s00442-011-2173-z
- Lamarque, J. F., Dentener, F., McConnell, J., Ro, C. U., Shaw, M., Vet, R., Bergmann, D., Cameron-Smith, P., Dalsoren, S., Doherty, R., Faluvegi, G., Ghan, S. J., Josse, B., Lee, Y. H., MacKenzie, I. A., Plummer, D., Shindell, D. T., Skeie, R. B., Stevenson, D. S., ... Nolan, M. (2013). Multi-model mean nitrogen and sulfur deposition from the atmospheric chemistry and climate model intercomparison project (ACCMIP): Evaluation of historical and projected future changes. Atmospheric Chemistry and Physics, 13, 7997–8018. https://doi.org/10.5194/acp-13-7997-2013
- Lauber, C. L., Hamady, M., Knight, R., & Fierer, N. (2009). Pyrosequencingbased assessment of soil pH as a predictor of soil bacterial community structure at the continental scale. Applied and Environmental Microbiology, 75, 5111–5120. https://doi.org/10.1128/AEM.00335-09
- Lavallee, J. M., Soong, J. L., & Cotrufo, M. F. (2020). Conceptualizing soil organic matter into particulate and mineral—Associated forms to address global change in the 21st century. Global Change Biology, 26, 261–273. https://doi.org/10.1111/gcb.14859
- Li, J., Sang, C., Yang, J., Qu, L., Xia, Z., Sun, H., Jiang, P., Wang, X., He, H., & Wang, C. (2021). Stoichiometric imbalance and microbial community regulate microbial elements use efficiencies under nitrogen addition. Soil Biology and Biochemistry, 156, 108207. https://doi. org/10.1016/j.soilbio.2021.108207
- Liang, C., Schimel, J. P., & Jastrow, J. D. (2017). The importance of anabolism in microbial control over soil carbon storage. *Nature Microbiology*, 2, 17105. https://doi.org/10.1038/nmicrobiol.2017.105
- Lin, Y., Slessarev, E. W., Yehl, S. T., D'Antonio, C. M., & King, J. Y. (2019). Long-term nutrient fertilization increased soil carbon storage in California grasslands. *Ecosystems*, 22, 754–766. https://doi. org/10.1007/s10021-018-0300-y
- Ma, Q., Liu, X., Li, Y., Li, L., Yu, H., Qi, M., Zhou, G., & Xu, Z. (2020). Nitrogen deposition magnifies the sensitivity of desert steppe plant communities to large changes in precipitation. *Journal of Ecology*, 108, 598-610. https://doi.org/10.1111/1365-2745.13264
- Maestre, F. T., Eldridge, D. J., Soliveres, S., Kéfi, S., Delgado-Baquerizo, M., Bowker, M. A., García-Palacios, P., Gaitán, J., Gallardo, A.,

- Lázaro, R., & Berdugo, M. (2016). Structure and functioning of dryland ecosystems in a changing world. *Annual Review of Ecology, Evolution, and Systematics*, 47, 215–237. https://doi.org/10.1146/annurev-ecolsys-121415-032311
- Manzoni, S., Taylor, P., Richter, A., Porporato, A., & Ågren, G. I. (2012). Environmental and stoichiometric controls on microbial carbonuse efficiency in soils. *New Phytologist*, 196, 79–91. https://doi.org/10.1111/j.1469-8137.2012.04225.x
- Marx, M.-C., Wood, M., & Jarvis, S. C. (2001). A microplate fluorimetric assay for the study of enzyme diversity in soils. *Soil Biology and Biochemistry*, 33, 1633–1640.
- Niu, G., Wang, R., Hasi, M., Wang, Y., Geng, Q., Wang, C., Jiang, Y., & Huang, J. (2021). Availability of soil base cations and micronutrients along soil profile after 13-year nitrogen and water addition in a semi-arid grassland. *Biogeochemistry*, 152, 223–236. https://doi. org/10.1007/s10533-020-00749-5
- Ochoa-Hueso, R., Maestre, F. T., de Los Ríos, A., Valea, S., Theobald, M. R., Vivanco, M. G., Manrique, E., & Bowker, M. A. (2013). Nitrogen deposition alters nitrogen cycling and reduces soil carbon content in low-productivity semiarid Mediterranean ecosystems. *Environmental Pollution*, 179, 185–193. https://doi.org/10.1016/j.envpol.2013.03.060
- Osborne, B. B., Bestelmeyer, B. T., Currier, C. M., Homyak, P. M., Throop, H. L., Young, K., & Reed, S. C. (2022). The consequences of climate change for dryland biogeochemistry. *New Phytologist*, 236, 15–20. https://doi.org/10.1111/nph.18312
- O'Sullivan, M., Spracklen, D. V., Batterman, S. A., Arnold, S. R., Gloor, M., & Buermann, W. (2019). Have synergies between nitrogen deposition and atmospheric CO₂ driven the recent enhancement of the terrestrial carbon sink? *Global Biogeochemical Cycles*, 33, 163–180. https://doi.org/10.1029/2018GB005922
- Parolari, A. J., Goulden, M. L., & Bras, R. L. (2012). Fertilization effects on the ecohydrology of a southern California annual grassland. Geophysical Research Letters, 39, L08405. https://doi.org/10.1029/2012GL051411
- Plaza, C., Gascó, G., Méndez, A. M., Zaccone, C., & Maestre, F. T. (2018). Soil organic matter in dryland ecosystems. In C. Garcia, P. Nannipieri, & T. Hernandez (Eds.), The future of soil carbon Its conservation and formation (1st ed., pp. 39–70). Elsevier. https://doi.org/10.1016/B978-0-12-811687-6/00002-X
- Plaza, C., Zaccone, C., Sawicka, K., Méndez, A. M., Tarquis, A., Gascó, G., Heuvelink, G. B. M., Schuur, E. A. G., & Maestre, F. T. (2018). Soil resources and element stocks in drylands to face global issues. *Scientific Reports*, 8, 13788. https://doi.org/10.1038/s41598-018-32229-0
- Poeplau, C., Don, A., Six, J., Kaiser, M., Benbi, D., Chenu, C., Cotrufo, M. F., Derrien, D., Gioacchini, P., Grand, S., Gregorich, E., Griepentrog, M., Gunina, A., Haddix, M., Kuzyakov, Y., Kühnel, A., Macdonald, L. M., Soong, J., ... Nieder, R. (2018). Isolating organic carbon fractions with varying turnover rates in temperate agricultural soils—A comprehensive method comparison. Soil Biology and Biochemistry, 125, 10–26. https://doi.org/10.1016/j.soilbio.2018.06.025
- Poeplau, C., Helfrich, M., Dechow, R., Szoboszlay, M., Tebbe, C. C., Don, A., Greiner, B., Zopf, D., Thumm, U., Korevaar, H., & Geerts, R. (2019). Increased microbial anabolism contributes to soil carbon sequestration by mineral fertilization in temperate grasslands. *Soil Biology and Biochemistry*, 130, 167–176. https://doi.org/10.1016/j.soilbio.2018.12.019
- Pold, G., Domeignoz-Horta, L. A., Morrison, E. W., Frey, S. D., Sistla, S. A., & Deangelis, K. M. (2020). Carbon use efficiency and its temperature sensitivity covary in soil bacteria. mBio, 11, e02293-19. https:// doi.org/10.1128/mBio.02293-19
- Potts, D. L., Suding, K. N., Winston, G. C., Rocha, A. V., & Goulden, M. L. (2012). Ecological effects of experimental drought and prescribed fire in a southern California coastal grassland. *Journal*

- of Arid Environments, 81, 59-66. https://doi.org/10.1016/j.jaridenv.2012.01.007
- Prăvălie, R. (2016). Drylands extent and environmental issues. A global approach. *Earth-Science Reviews*, 161, 259–278. https://doi.org/10.1016/j.earscirev.2016.08.003
- Püspök, J. F. (2022). Effects of experimental nitrogen deposition on dryland soil organic carbon storage. Retrieved September 20, 2022, from 10.17605/OSF.IO/W78VD.
- Qi, Y., Wei, W., Chen, C., & Chen, L. (2019). Plant root-shoot biomass allocation over diverse biomes: A global synthesis. *Global Ecology and Conservation*, 18, e00606. https://doi.org/10.1016/j.gecco.2019.e00606
- Rasmussen, C., Heckman, K., Wieder, W. R., Keiluweit, M., Lawrence, C.
 R., Asefaw, A., Blankinship, J. C., Crow, S. E., Druhan, J. L., Pries,
 C. E. H., Marin-Spiotta, E., Plante, A. F., Schädel, C., Schimel, J. P.,
 Sierra, C. A., Thompson, A., Wagai, R., & Christina, F. P. (2018).
 Beyond clay: Towards an improved set of variables for predicting
 soil organic matter content. *Biogeochemistry*, 137, 297–306. https://doi.org/10.1007/s10533-018-0424-3
- Riggs, C. E., & Hobbie, S. E. (2016). Mechanisms driving the soil organic matter decomposition response to nitrogen enrichment in grassland soils. *Soil Biology and Biochemistry*, *99*, 54–65. https://doi.org/10.1016/j.soilbio.2016.04.023
- Rodhe, H., Dentener, F., & Schulz, M. (2002). The global distribution of acidifying wet deposition. Environmental Science and Technology, 36, 4382–4388. https://doi.org/10.1021/es020057g
- Rossel, Y. (2012). lavaan: An R package for structural equation modeling. *Journal of Statistical Software*, 48, 1–36.
- Rossi, L. M. W., Mao, Z., Merino-Martín, L., Roumet, C., Fort, F., Taugourdeau, O., Boukcim, H., Fourtier, S., Rey-Granado, M., Chevallier, T., Cardinael, R., Fromin, N., & Stokes, A. (2020). Pathways to persistence: Plant root traits alter carbon accumulation in different soil carbon pools. *Plant and Soil*, 452, 457–478. https://doi.org/10.1007/s11104-020-04469-5
- Rowley, M. C., Grand, S., & Verrecchia, É. P. (2018). Calcium-mediated stabilisation of soil organic carbon. *Biogeochemistry*, 137, 27–49. https://doi.org/10.1007/s10533-017-0410-1
- Satorra, A., & Bentler, P. M. (1994). Corrections to test statistics and standard errors in covariance structure analysis. In A. Eye & C. C. Clogg (Eds.), Latent variables analysis: Applications for developmental research (pp. 399–419). Sage.
- Schaeffer, S. M., Billings, S. A., & Evans, R. D. (2003). Responses of soil nitrogen dynamics in a Mojave Desert ecosystem to manipulations in soil carbon and nitrogen availability. *Oecologia*, 134, 547–553. https://doi.org/10.1007/s00442-002-1130-2
- Schimel, J. P. (2018). Life in dry soils: Effects of drought on soil microbial communities and processes. *Annual Review of Ecology, Evolution, and Systematics*, 49, 409–432. https://doi.org/10.1146/annurev-ecolsys-110617-062614
- Slessarev, E. W., Lin, Y., Bingham, N. L., Johnson, J. E., Dai, Y., Schimel, J. P., & Chadwick, O. A. (2016). Water balance creates a threshold in soil pH at the global scale. *Nature*, 540, 567–569. https://doi.org/10.1038/nature20139
- Sokol, N. W., & Bradford, M. A. (2019). Microbial formation of stable soil carbon is more efficient from belowground than aboveground input. *Nature Geoscience*, 12, 46–53. https://doi.org/10.1038/ s41561-018-0258-6
- Sokol, N. W., Sanderman, J., & Bradford, M. A. (2019). Pathways of mineral—Associated soil organic matter formation: Integrating the role of plant carbon source, chemistry, and point of entry. Global Change Biology, 25, 12–24. https://doi.org/10.1111/gcb.14482
- Soong, J. L., & Cotrufo, M. F. (2015). Annual burning of a tallgrass prairie inhibits C and N cycling in soil, increasing recalcitrant pyrogenic organic matter storage while reducing N availability. Global Change Biology, 21, 2321–2333. https://doi.org/10.1111/gcb.12832

- Su, J., Li, X., Li, X., & Feng, L. (2013). Effects of additional N on herbaceous species of desertified steppe in arid regions of China: A four-year field study. Ecological Research, 28, 21–28. https://doi.org/10.1007/ s11284-012-0994-9
- Throop, H. L., & Belnap, J. (2019). Connectivity dynamics in dryland litter cycles: Moving decomposition beyond spatial stasis. Bioscience, 69. 602-614. https://doi.org/10.1093/biosci/biz061
- Tian, D., & Niu, S. (2015). A global analysis of soil acidification caused by nitrogen addition. Environmental Research Letters, 10, 024019. https://doi.org/10.1088/1748-9326/10/2/024019
- Treseder, K. K. (2008). Nitrogen additions and microbial biomass: A meta-analysis of ecosystem studies. Ecology Letters, 11, 1111-1120. https://doi.org/10.1111/j.1461-0248.2008.01230.x
- Valliere, J. M., Irvine, I. C., Santiago, L., & Allen, E. B. (2017). High N, dry: Experimental nitrogen deposition exacerbates native shrub loss and nonnative plant invasion during extreme drought. Global Change Biology, 23, 4333-4345. https://doi.org/10.1111/gcb.13694
- Vance, E. D., Brookes, P. C., & Jenkinson, D. S. (1987). An extraction method for measuring soil microbial biomass C. Soil Biology and Biochemistry, 19(6), 703-707. https://doi. org/10.1016/0038-0717(87)90052-6
- Vourlitis, G. L. (2012). Aboveground net primary production response of semi-arid shrublands to chronic experimental dry-season N input. Ecosphere, 3(3), 22. https://doi.org/10.1890/ES11-00339.1
- Vourlitis, G. L., Jaureguy, J., Marin, L., & Rodriguez, C. (2021). Shoot and root biomass production in semi-arid shrublands exposed to longterm experimental N input. Science of the Total Environment, 754, 142204. https://doi.org/10.1016/j.scitotenv.2020.142204
- Vourlitis, G. L., Kirby, K., Vallejo, I., Asaeli, J., & Holloway, J. M. (2021). Potential soil extracellular enzyme activity is altered by longterm experimental nitrogen deposition in semiarid shrublands. Applied Soil Ecology, 158, 103779. https://doi.org/10.1016/j. apsoil.2020.103779
- Wan, D., Ma, M., Peng, N., Luo, X., Chen, W., Cai, P., Wu, L., Pan, H., Chen, J., Yu, G., & Huang, Q. (2021). Effects of long-term fertilization on calcium-associated soil organic carbon: Implications for C sequestration in agricultural soils. Science of the Total Environment, 772, 145037. https://doi.org/10.1016/j.scitotenv.2021.145037
- Weil, R. R., & Brady, N. C. (2017). The nature and properties of soils (15th ed.). Pearson Education.
- Whalen, E. D., Grandy, A. S., Sokol, N. W., Keiluweit, M., Ernakovich, J., Smith, R. G., & Frey, S. D. (2022). Clarifying the evidence for microbial- and plant-derived soil organic matter, and the path toward a more quantitative understanding. Global Change Biology, 28, 7167-7185. https://doi.org/10.1111/gcb.16413
- Wobbrock, J. O., Findlater, L., Gergle, D., & Higgins, J. J. (2011). The aligned rank transformation for nonparametric factorial analyses using only ANOVA procedures. In CHI '11: Proceedings of the SIGCHI conference on human factors in computing systems (pp. 143-146). Association for Computing Machinery.

- Wolkovich, E. M., Lipson, D. A., Virginia, R. A., Cottingham, K. L., & Bolger, D. T. (2010). Grass invasion causes rapid increases in ecosystem carbon and nitrogen storage in a semiarid shrubland. Global Change Biology, 16, 1351-1365. https://doi. org/10.1111/j.1365-2486.2009.02001.x
- Xu. C., Xu. X., Ju. C., Chen. H. Y. H., Wilsey, B. J., Luo, Y., & Fan. W. (2021). Long-term, amplified responses of soil organic carbon to nitrogen addition worldwide. Global Change Biology, 27, 1170-1180. https:// doi.org/10.1111/gcb.15489
- Yahdjian, L., Gherardi, L., & Sala, O. E. (2011). Nitrogen limitation in arid-subhumid ecosystems: A meta-analysis of fertilization studies. Journal of Arid Environments, 75, 675-680. https://doi. org/10.1016/j.jaridenv.2011.03.003
- Yang, Y., Ji, C., Ma, W., Wang, S., Wang, S., Han, W., Mohammat, A., Robinson, D., & Smith, P. (2012). Significant soil acidification across northern China's grasslands during 1980s-2000s. Global Change Biology, 18, 2292-2300. https://doi. org/10.1111/j.1365-2486.2012.02694.x
- Ye, C., Chen, D., Hall, S. J., Pan, S., Yan, X., Bai, T., Guo, H., Zhang, Y., Bai, Y., & Hu, S. (2018). Reconciling multiple impacts of nitrogen enrichment on soil carbon: Plant, microbial and geochemical controls. Ecology Letters, 21, 1162-1173. https://doi.org/10.1111/ ele.13083
- Zak, D. R., Argiroff, W. A., Freedman, Z. B., Upchurch, R. A., Entwistle, E. M., & Romanowicz, K. J. (2019). Anthropogenic N deposition, fungal gene expression, and an increasing soil carbon sink in the Northern Hemisphere. Ecology, 100, e02804. https://doi.org/10.1002/ ecy.2804
- Zeng, D.-H., Li, L.-J., Fahey, T. J., Yu, Z.-Y., Fan, Z.-P., & Chen, F.-S. (2010). Effects of nitrogen addition on vegetation and ecosystem carbon in a semi-arid grassland. Biogeochemistry, 98, 185-193. https://doi. org/10.1007/s10533-009-9385-x

SUPPORTING INFORMATION

Additional supporting information can be found online in the Supporting Information section at the end of this article.

How to cite this article: Püspök, J. F., Zhao, S., Calma, A. D., Vourlitis, G. L., Allison, S. D., Aronson, E. L., Schimel, J. P., Hanan, E. J., & Homyak, P. M. (2023). Effects of experimental nitrogen deposition on soil organic carbon storage in Southern California drylands. Global Change Biology, 29, 1660-1679. https://doi.org/10.1111/gcb.16563